Mechanistic Modeling of Biodiesel Production via Heterogeneous Catalysis

Nuttapol Lerkkasemsan

Thesis submitted to the faculty of the Virginia Polytechnic Institute and State University in partial fulfillment of the requirements for the degree of

Master of Science

In

Chemical Engineering

Luke Achenie(Chair)

Foster Agblevor

David F. Cox

May 4, 2010

Blacksburg, Virginia

Keywords: deterministic modeling, stochastic modeling, free fatty acid esterification, biodiesel, Eley-Rideal

Mechanistic Modeling of Biodiesel Production via Heterogeneous Catalysis

Nuttapol Lerkkasemsan

ABSTRACT

Biodiesel has emerged as a promising renewable and clean energy alternative to petrodiesel. While biodiesel has traditionally been prepared through homogeneous basic catalysis, heterogeneous acid catalysis has been investigated recently due to its ability to convert cheaper but high free fatty acid content oils such as waste vegetable oil while decreasing production cost. In this work, the esterification of free fatty acid over sulfated zirconia and activated acidic alumina in a batch reactor was considered. The models of the reaction over the catalysts were developed in two parts. First, a kinetic study was performed using a deterministic model to develop a suitable kinetic expression; the related parameters were subsequently estimated by numerical techniques. Second, a stochastic model was developed to further confirm the nature of the reaction at the molecular level. The esterification of palmitic acid obeyed the Eley-Rideal mechanism in which palmitic acid and methanol are adsorbed on the surface for SO_4/ZrO_2-550°C and $AcAl_2O_3$ respectively. The coefficients of determination of the deterministic model were 0.98, 0.99 and 0.99 for SO_4/ZrO_2-550°C at 40, 60 and 80°C respectively and 0.99, 0.98 and 0.96 for $AcAl_2O_3$

at the same temperature. The deterministic and stochastic models were in good agreement.

Acknowledgement

The authors duly acknowledge the Institute for Critical Technology and Applied Science at Virginia Polytechnic Institute and State University for funding this project. The experimental studies were conducted by Nourredine Abdoulmoumine in Dr. Agblevor's lab in Biological Systems Engineering.

Table of contents

List of Figures

List of Tables

Chapter 1 Introduction

In recent years, biodiesel has been shown to be a promising alternative renewable energy source for petrol-diesel. As a result biodiesel production has been increasingly investigated by many scientists. This upward increase in interest was prompted by environmental concerns of global warming and the mounting evidence of the depletion of natural crude oil reserves. At the current usage rate, petroleum reserves will be depleted by the end of the next century (Pryde,1983, Shafiee and Topal,2009). Biodiesel is gentler on the environment. For example, biodiesel is biodegradable and is also carbon neutral (Kulkarni, et al.,2006) because it is produced from renewable sources such as vegetable oil and animal fat.

The traditional method of biodiesel production is through the esterification of vegetable oil and animal fat with alcohol using homogeneous catalysts such as NaOH or KOH. However, homogeneous basic catalysts are susceptible to free fatty acid (FFA) and water which are found in cheaper feedstock such as waste cooking oil. The homogeneous basic catalysts can react with the free fatty acid to form soap through saponification reaction. The water in feedstock can promote reverse reaction to take place between the product. Therefore, even if the homogeneous basic catalysts can achieve a high yield of Fatty Acid Methyl Ester (FAME), it limits the choice of feedstock. One solution to this problem is to use homogeneous acid catalysts to convert FFA before using homogeneous basic catalysts. However, the

homogeneous acid catalysts have a problem of corrosion. To solve these entire problems, the heterogeneous acid catalysts have been developed. It can simultaneously react with both FFA and triacylglycerols. Moreover, it can be easily separated from product and reused for several times. These advantages can reduce biodiesel production cost that can make biodiesel price competitive with petrol diesel. The heterogeneous acid catalysts which were studied in this research are SO_4/ZrO_2 and $AcAl_2O_3$.

Chapter 2 Literature Review

There are several methods in biodiesel production; the following section will outline a few of those methods.

Biodiesel making process

There are several ways to make biodiesel as follows:

1. Direct use of pure vegetable oil or blending with petrol-diesel in various ratios.
2. Microemulsions with solvent by blending diesel fuel with solvent such as alcohol.
3. Thermal cracking to alkane, alkenes, alkadines, etc.
4. Transesterification with catalyst

2.1. Direct use and blending

The direct use of vegetable oil in diesel engine was tested by Rudolph Diesel who was the inventor of diesel engine(Shay,1993). Because of low cost petrol-diesel at that time, using vegetable oil in diesel engine was not pursued. At the beginning of the 1980s, Batholomew et al (1981) addressed the concept of using food for fuel, indicating that food products such as vegetable oil, alcohol and some other forms of renewable resources should be the alternative fuel rather than petroleum. The most advanced work with sunflower seed oil occurred in South Africa because of the oil embargo.

Caterpilar Brazil, in 1980, used pre-combustion chamber engines with a mixture of 10% vegetable oil with petrol-diesel in

order to maintain total power without any modifications or adjustments of the engine. At that point, it was not practical to substitute 100% vegetable oil for diesel fuel, but a blend of 20% vegetable oil and 80% diesel fuel was successful.

A blend of 95% used cooking oil and 5% diesel fuel was used power the engines of a fleet of buses in the early 1980s ([Anon],1982). Blending or preheating was needed in order to compensate for cooler ambient temperatures. Incidentally, there were no coking and carbon build-up problems in this operation. The key to success was suggested to be filtering and the only problem reported was lubricating oil contamination. The viscosity of lubricating oil increased due to polymerization of polyunsaturated vegetable oils. The lubricating oil had to be changed between 4,000 and 4,500 miles.

Mixtures of degummed soybean oil and petrol-diesel fuel in the ratios of 1:2 and 1:1 were tested(Adams, et al.,1983). The thickening and potential gelling of the lubricant existed for the 1:1 blend, but it did not occur with the 1:2 blend. The results indicated that the 1:2 blends should be suitable as fuel for agricultural equipment during periods of diesel fuel shortages.

Two severe problems associated with the use of vegetable oils (directly or blended with petrol-diesel fuels) were oil deterioration and incomplete combustion(Peterson, et al.,1983). Polyunsaturated fatty acids were very susceptible to polymerization, gum formation caused by oxidation during storage or by complex oxidative, thermal polymerization at the higher

temperature and pressure of combustion. The gum did not combust completely, resulting in carbon deposits and lubricating oil thickening.

According to Pryde et al, the advantages of direct use and blending vegetable oils in diesel fuel are(1983):

1. Portability (Liquid fuel)
2. Heat content (88% of diesel no.2 fuel)
3. Ready availability
4. Renewability
5. Lower sulfur and aromatic content

The disadvantages are:

I. Higher viscosity
II. Lower volatility
III. The reactivity of unsaturated hydrocarbon chains

there are several problems that appear after long periods of time, especially with direct-injection engines(Ma and Hanna,1999). The problems are listed below:

1. Carbon deposit
2. Thickening and gelling of the lubricating oil as a result of contamination by vegetable oils
3. Coking and trumpet formation on the injectors to such an extent that fuel atomization does not occur properly or is even prevented as a result of plugged orifices
4. Lubricating problems
5. Oil ring sticking

In addition, the vegetable oil and animal fats also have high viscosity which is 11 to 17 times higher than petroleum diesel. They also have lower volatilities which causes incomplete combustion. In addition, vegetable oil can form large agglomerations which are caused by the polymerization of unsaturated fatty acids at high temperature as well as gumming. This problem occurs because vegetable oil contains a lot of unsaturated fatty acids. Because of these problems, the direct use and blending methods are not popular.

2.2. Microemulsions

The main idea of creating microemulsions is to try to reduce the viscosity of vegetable oil with solvents such as methanol, ethanol, and 1-butanol. This method can eliminate the problem of high viscosity that plagues vegetable oil. (Schwab, et al.,1987). A microemulsion is a system of water, oil, and amphiphilic compounds (surfactant and co-surfactant); it is a transparent, single optically isotropic, and thermodynamically stable liquid.

Ziejewski et al.(1984) prepared an emulsion of 53.3% (v/v) alkali-reined and winterized sunflower oil, 13.3% (v/v) 1-butanol. This non-ionic emulsion had a viscosity of $6.31 \times 10^{-6} \frac{m^2}{s}$ at 40°C, a cetane number of 25, sulfur content of 0.01%, free fatty acids of 0.01%, and ash content of less than 0.01%. Lower viscosities and better spray patterns were obtained by increasing the amount of 1-butanol. Short term performances of both ionic and non-ionic microemulsions of aqueous ethanol in soy bean oil

were nearly as good as that of No.2 diesel, despite the lower cetane number and energy content. However, there are still problems after using this fuel for a long term. Problems such as injector needle sticking, carbon deposits, incomplete combustion, and increasing viscosity of lubricating oils were reported(Ma and Hanna,1999).

2.3. Thermal Cracking (Pyrolysis)

Thermal cracking or pyrolysis involves heating in the absence of air or oxygen and cleavage of chemical bonds to yield small molecule (WEISZ, et al.,1979). This is often done with the aid of a catalyst (Ma and Hanna,1999). The first pyrolysis of vegetable oil was conducted in China in an attempt to synthesize petroleum from vegetable oil during World War II.

Pyrolysis chemistry is difficult to characterize because of the variety of reaction paths and the variety of reaction products that may be obtained from the reactions that take place. Many investigators have studied the pyrolysis of triglycerides with the aim of obtaining products suitable for diesel engines (Alencar, et al.,1983, Billaud, et al.,1995, Crossley, et al.,1962, Schwab, et al.,1988). The pyrolyzed material can be vegetable oils, animal fats, natural fatty acids, and methyl esters of fatty acids. The products include alkanes, alkenes, alkadienes, aromatics, and carboxylic acids. The mechanisms for the thermal decomposition of a triglyceride are given in Figure 1.

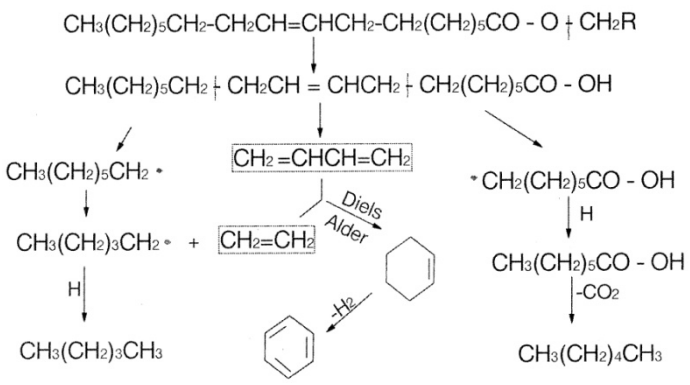

Figure 1: The mechanism of thermal decomposition of triglycerides (Schwab, et al.,1988)

Different types of vegetable oils reveal large differences in composition when they are thermally decomposed. For example, pyrolyzed soybean oil contains 79% carbon and 12% hydrogen(Schwab, et al.,1988). The biodiesel produced in this process has low viscosity and a high cetane number compared to pure vegetable oils. Moreover, pyrolyzed vegetable oil has acceptable amounts of sulfur, water and sediment. However, they are unacceptable in terms of ash, carbon residues, and pour points. The equipment of thermal cracking or pyrolysis is expensive for modest throughputs. In addition, while the products are chemically similar to petroleum-derived gasoline and diesel fuel, the removal of oxygen during the thermal processing also removes any environmental benefits of using an oxygenated fuel (Ma and Hanna,1999). It also produced some low value material.

2.4. Transesterification

Biodiesel could be produced by the transesterification of triacylglycerols through base catalysis (Figure 2) or

esterification of free fatty acids and triacylglycerols by acid catalysis (Figure 3).

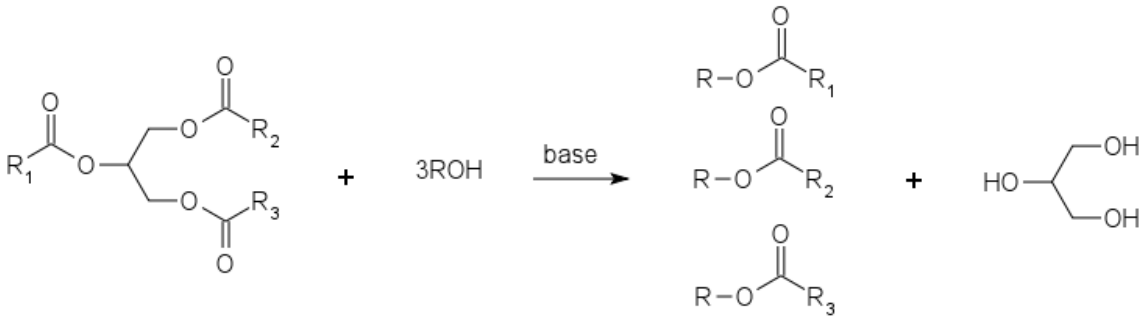

Figure 2: Transesterification of triacylglycerol to produce three fatty acid alkyl esters by base catalysis

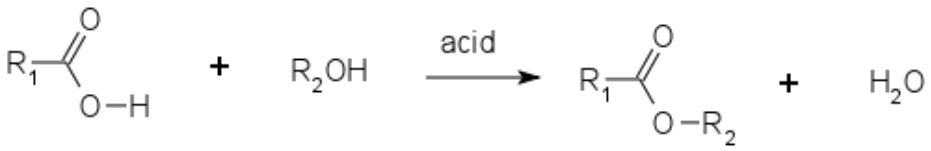

Figure 3: Esterification of a free fatty acid to an alkyl fatty acid ester by acid catalysis

The most common catalyst for both esterification and transesterification reaction are homogeneous catalyst, especially homogeneous basic catalysts. Vicente et al (2004) reported the transesterification of sunflower seed oil and methanol at 65°C using four different homogeneous basic catalysts, namely sodium hydroxide, potassium hydroxide, sodium methoxide, and potassium methoxide. The ratio of methanol per sunflower oil was 6:1 with

1wt% of catalyst. The report showed that the biodiesel yield after the separation process and purification process were higher than 98 wt% for the methoxide catalysts, because the yield losses due to triglyceride saponification and methyl ester dissolution in glycerol were negligible. The biodiesel yield for the sodium and potassium hydroxide were lower, 85.9 and 91.67 wt% respectively. However, the cost of methoxide catalysts is higher than hydroxide catalysts and also more difficult to manipulate since they are very hygroscopic. Therefore, applications that employ homogeneous catalysts prefer sodium or potassium hydroxide because they are inexpensive compared to methoxide. Moreover, sodium hydroxide is the fastest catalyst, in the sense that it achieves 100 wt% of methyl ester concentration in the biodiesel phase in just 30 minutes. Unfortunately, when a basic homogeneous catalyst is used for the transesterification of feeds with FFAs, soaps are produced as by-products through the unwanted saponification reaction of carboxylic acids with the base catalyst (Pasias, et al.,2006).

$$ROOH + NaOH \text{ (or } MeONa) \rightarrow ROO^{-}Na^{+} + H_2O \text{ (or } MeOH) \quad (1.1)$$

$$ROOMe + H_2O \Leftrightarrow ROOH + MeOH \quad (1.2)$$

The water that is produced by hydrolysis (1.1) reacts with the esters to form more FFA that consumes the base catalyst to produce soap, according to reaction (1.2). Because of these problems, homogeneous basic catalysts are susceptible to water and FFA, which are found in cheap feedstock such as waste cooking oil. Therefore, homogeneous basic catalysts are more suitable for

refined vegetable oil, which can raise the production cost of biodiesel. This means that the cost of biodiesel cannot be lower to be competitive with petrol-diesel because of high price feedstock. Moreover, the homogeneous basic catalysts are also nonrenewable catalysts.

Several methods have been proposed to solve these problems, but the most useful method seems to be pre-esterification with acid catalysis.

Pre-esterification method

The homogeneous acid catalyzed pre-esterification of FFA is a common practice in reducing FFA levels in feedstock with high FFA, before performing the base catalysts transesterification (Kulkarni and Dalai,2006, Lotero, et al.,2005). The disadvantage of the pre-esterification method consists of the necessity to remove the homogeneous acid catalyst from the oil after pre-esterification. To improve the process, the solution is the use of a heterogeneous esterification catalyst(Lotero, et al.,2005). The biodiesel production process by pre-esterification method is shown in (Figure 4).

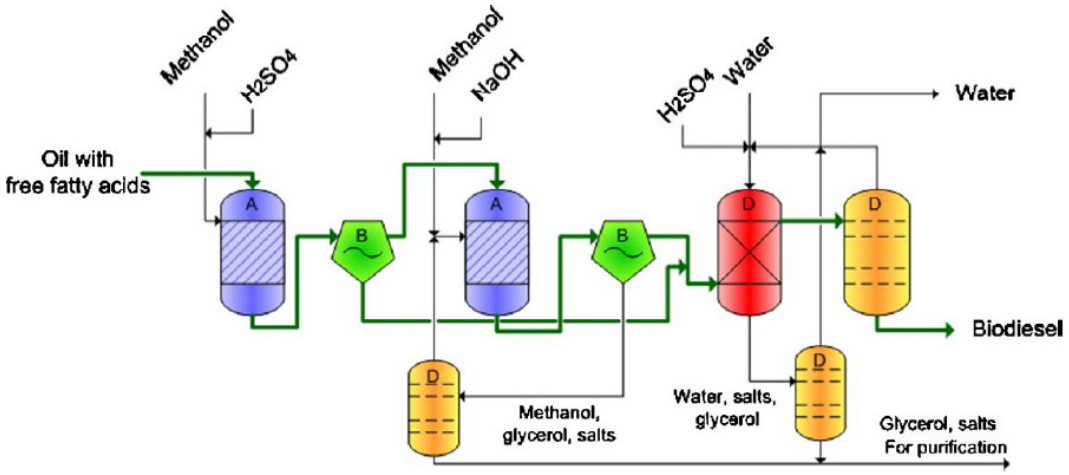

Figure 4: Traditional biodiesel processes with an acidic pre treatment step followed by alkaline catalysis. (A) Reactor; (B) Separation (centrifuge or decanter); (D) Product purification and alcohol recovery (Fjerbaek, et al.,2009)

Use of acid catalysts

Homogeneous acid catalyst is technically feasible and less complex than a two-step process, which is pre-esterification with homogeneous acid catalyst followed by alkali-catalysis (Zhang, et al.,2003). However, this process is associated with problems linked with the corrosive nature of the liquid acid catalyst and to the high quantity of byproduct obtained (Di Serio, et al.,2005). There is a way to perform triglyceride transesterification and FFA esterification in a single step, using low concentrations of a homogeneous Lewis acid catalyst. However, this process also has its shortcomings linked to the need to remove catalysts from products by downstream purification (Di Serio, et al.,2005). A solid acid catalyst could solve these problems (Lotero, et al.,2005).

Heterogeneous Catalysts

The use of heterogeneous catalysts can easily solve the problem of separation of products and catalysts after the esterification reaction. There are two types of heterogeneous catalysts. The first one is heterogeneous basic catalysts such as MgO and hydrotalcites (CHT). The second one is heterogeneous acid catalysis such as titanium oxide supported on silica, TiO_2/SiO_2 (TS); Vanadyl phosphate $VOPO_4 \cdot 2H_2O$ (VOP) and metal-substituted Vanadyl Phosphate $Me(H_2O)xVO(1-x)PO_4 \cdot 2H_2O$ (MeVOP). Di Serio et al (2007)studied both basic and heterogeneous acid catalysts, namely MgO, CHT, TS, VOP and MeVOP. The study shows that MgO and CHT have high activities. However, in the presence of FFAs both catalysts form soap during the reactions because of saponification reaction. Therefore, the heterogeneous basic catalyst is also vulnerable for the same reasons as the homogeneous basic catalysts. On the other hand, the solid acid catalysts are poorly affected by the presence of FFAs. Therefore, the solid acid catalysts can be useful for producing biodiesel from low quality feedstock which contain substantial amount of FFAs such as waste cooking oil. Using cheaper feedstock without having to refine it can lead to the reduction in the cost of biodiesel production. Furthermore, heterogeneous catalysis enables a continuous and flexible process implementation the reaction in a continuous fixed bed catalytic reactor. The utilization of heterogeneous catalyst thus means more flexibility and less downstream separation. It also means less catalyst replacements in the fixed bed catalytic reactor, which leads to a

higher quality of the final biodiesel product (Gomes, et al.,2008). Furthermore, heterogeneous catalysis results in cleaner glycerol, which further improves the profitability of the process. The absence of the alkaline catalyst neutralization step and the necessity to replace the consumed catalyst can simplify the production line and reduce the cost of production.

The performances of several heterogeneous catalysts are shown in Table 1.

Table 1:Published results on heterogeneous catalyst, experimental conditions and respective results obtained, found in literature research, for biodiesel production (Gomes, et al.,2008)

Catalysts	Results	Reference
ZrO_2/SO_4^{2-}	Good results in the reaction conversion and yield for ZrO_2/SO_4^{2-}, in a large range of temperatures	(Kiss, et al.,2006)
Dibutyltin oxide $((C_4H_9)_2SnO)$	Soya oil transesterification. Molar ratio oil/methanol/catalyst: 100/400/1, 10 hours of residence reaction time. Higher conversion (35%) for dibutyltin oxide.	(Rosa and Oliveira,2005)
Supported catalysts Fe-Zn in cyanid	Higher activity and selectivity using complex	(Srivastava, et al.,2006)

complexes, with and without t-buthanol (complex agent) and with a co-polymer ($EO_{20}PO_{70}EO_{20}$)	agent in the catalytic matrix	
SiO_2/H_2SO_4, SiO_2/KOH and Al_2O_3/KOH, SiO_2/HCl, $SiO_2/ZnCl_2$, SiO_2/ Al_2O_3 and Al_2O_3/ H_2SO_4	Mamona and soy oil transesterification, with methanol, temperatures of 25C and 65C, ratio support/catalyst of 50%(w/w), rati oil/methanol of 1:6, mass ratio of 5g oil/0.25g of catalyst. Best results for supported alumina catalysts for alkaline catalysis. While the silica catalysts showed best results for acid catalysis.	(Perin, et al.,2006)
K_2CO_3, Na_2CO_3 and $CaCO_3$	Mamona oil transesterification with methanol, ratio oil/methanol/catalyst of 100/600/1. Reaction time of 10 hours. K_2CO_3 showed	(Rosa and Oliveira,2006)

	best catalystic activity and higher yields in biodiesel production. $CaCO_3$ did not show any catalytic activity.	
Zeolite Y	Employment of used fried oils. Good biodiesel yield.	(Brito, et al.,2007)
ZrO_2/SO_4^{2-}	Good results at catalyst activity and in the biodiesel yield production	(West, et al.,2007)
Hydrotalcites of Mg and Al (ratio Mg/Al of 3). Modified with Zn, Sn, Ba, Mn, Ce and Ca, with 5% catalyst (wt.%)	Soy oil transesterification with methanol, 70C, reaction time of 3 hours, ratio methanol/oil of 9:1. Good results regarding biodiesel yield and product quality.	(Santos,2007)

In the present work, the Eley-Rideal model has been shown to be suitable for studying the kinetics of palmitic acid esterification on sulfated zirconium oxide and activated acidic alumina catalysts. Furthermore, the Gillespie model was used to investigate the consistency of the model.

Chapter 3 Experiments

(The experiments were conducted in the Department of Biological Systems Engineering by Nourredine Abdoulmoumine, a collaborating graduate student.)

3.1 Materials

Zirconium oxide and activated acidic alumina were obtained from Alfa Aeasar (Alfa Aesar, Ward Hill, MA). Palmitic acid was purchased from Sigma Aldrich (St. Louis, MO). Methanol, n-hexane and acetonitrile were all purchased from Fischer Scientific (Fair Lawn, NJ) as analytical grade solvents and used as received.

3.2 Catalyst preparation and characterization

Zirconium oxide was ground to pass through a 20 mesh and subsequently sulfated according to the procedure described by Arata (1996). After sulfation by incipient impregnation, the catalyst was activated at 550°C for 6h and this material was labeled as SO_4/ZrO_2-550°C. The activated acidic alumina catalyst was used as received without sulfation but was calcined at 550°C for 3h before use and was labeled as $AcAl_2O_3$. The sulfated zirconium oxide catalyst was characterized by XPS, SEM-EDS and BET. The acidic alumina catalyst was characterized by SEM-EDS for chemical composition and the surface area data was provided by the supplier.

3.3 Palmitic acid esterification

The reaction was carried in a water bath maintained at the appropriate temperature. In the reaction flask, 2.56g (0.01mol) of palmitic acid and 32.04g (1mol) of methanol were added and placed in the water bath first to reach temperature before adding the appropriate amount of catalyst. The free fatty acid to methanol content was increased 1:100 molar ratio to ensure complete immersion of palmitic acid in the reaction mixture. Furthermore, the higher methanol content prevented palmitic acid precipitation during sample collection improving the accuracy of the procedure.

Chapter 4 Deterministic kinetic models for transesterification reaction for palmitic acid

SO_4/ZrO_2-550°C and $AcAl_2O_3$ were used to perform the kinetic experiments at 40, 60 and 80°C at 10 wt% and 100 wt%. Eleven models (including Langmuir-Hinshelwood and Eley-Rideal models) were tested. The total active site on SO_4/ZrO_2-550°C was determined to be 2.05 wt%. For Alumina, due to the lack of actual experimental data, we employed literature total active site which was measured via chemisorption of ethylene on alumina; this was reported to be 35 %mole (Amenomiya and Cvetanovic,1970). It was assumed that an Eley-Rideal mechanism occurred with palmitic acid on the catalyst surface and reaction of bulk fluid methanol as the rate-determining step. For $AcAl_2O_3$ however, it was assumed that methanol was adsorbed on the catalyst surface and the palmitic acid was in the bulk fluid. The methanol adsorption was assumed as to be the rate- determining step.

4.1 Rate law Model

In chemical reaction, a power law model is the most popular model. However, rate laws in heterogeneous catalysis rarely follow power law models and hence are inherently more difficult to formulate from the data (Fogler,2006). In order to develop an in-depth understanding and in sight as to how the rate laws are formed from heterogeneous catalytic data, we will postulate catalytic mechanisms and derive rate laws for the various mechanisms. The mechanisms will typically have an adsorption

step, a surface reaction step, and a desorption step, one of which is usually a rate-determining step.

Knowing the different forms that catalytic rate equations can take, it will be easier to view the trends in the data and deduce the appropriate rate law. After knowing the form of the rate law, one can then numerically evaluate the rate law parameters and postulate a reaction mechanism and rate-determining step that is consistent with the rate data. Finally, one can use the rate law to design catalytic reactors.

To find a rate law for the esterification reaction, which occurs over the surface of the catalysts, we are going to use both the Langmuir-Hinshelwood model and the Eley-Rideal model. There are eleven models from the Langmuir-Hinshelwood and Eley-Rideal methods. The models are derived in the following sections.

4.1.1 Langmuir-Hinshelwood model

In this model, palmitic acid and methanol, which are the reactants, are adsorbed on the surface of the catalyst and react with each other. After the reaction, the products, which are water and biodiesel, are desorbed back to the bulk fluid. Therefore, the model can be formulated using the following equation:

$A + S \overset{k_{AB}, k_{-AB}}{\Longleftrightarrow} AS$ -Adsorption of palmitic acid (4.1.1-1)

$M + S \overset{k_{AM}, k_{-AM}}{\Longleftrightarrow} MS$ -Adsorption of methanol (4.1.1-2)

$AS + MS \overset{k_{S}, k_{-S}}{\Longleftrightarrow} ES + WS$ -Reaction of adsorbed species (4.1.1-3)

$ES \overset{k_{DB}k_{-DB}}{\Longleftrightarrow} E + S$ -Desorption of ester (4.1.1-4)

$WS \overset{k_{DW},k_{-DW}}{\Longleftrightarrow} W + S$ -Desorption of water (4.1.1-5)

Here the rate equations from reactions (4.1.1-1) to (4.1.1-5) can be written as below:

$-r_{AB} = k_{AB}\left(C_A C_v - \frac{C_{A\cdot S}}{K_{AB}}\right); K_{AB} = \frac{k_{AB}}{k_{-AB}}$ -Rate of adsorption of palmitic acid (4.1.1-6)

$-r_{AM} = k_{AM}\left(C_M C_v - \frac{C_{M\cdot S}}{K_{AM}}\right); K_{AM} = \frac{k_{AM}}{k_{-AM}}$ -Rate of adsorption of methanol (4.1.1-7)

$-r_S = k_S\left(C_{A\cdot S} C_{M\cdot S} - \frac{C_{E\cdot S} C_{W\cdot S}}{K_S}\right); K_S = \frac{k_S}{k_{-S}}$ -Rate of reaction of adsorbed species (4.1.1-8)

$-r_{DB} = k_{DB}\left(C_{E\cdot S} - \frac{C_E C_v}{K_{DB}}\right); K_{DB} = \frac{k_{DB}}{k_{-DB}}$ -Rate of desorption of ester (4.1.1-9)

$-r_{DW} = k_{DW}\left(C_{W\cdot S} - \frac{C_W C_v}{K_{DW}}\right); K_{DW} = \frac{k_{DW}}{k_{-DW}}$ -Rate of desorption of water (4.1.1-10)

The rate-determining step in the Langmuir-Hinshelwood model can be chosen in five ways.

I. The reaction of reactants is the rate-determining step. The k_{AB}, k_{AM}, k_{DB}, k_{DW} are large by comparison, and we can set.

$-\frac{r_{AB}}{k_{AB}} \cong 0$ $C_{A\cdot S} = K_{AB} C_A C_v$ (4.1.1-11)

$-\frac{r_{AM}}{k_{AM}} \cong 0$ $C_{M\cdot S} = K_{AM} C_M C_v$ (4.1.1-12)

$$-\frac{r_{DB}}{k_{DB}} \cong 0 \qquad C_{E\cdot S} = \frac{C_E C_v}{K_{DB}} \qquad (4.1.1\text{-}13)$$

$$-\frac{r_{DW}}{k_{DW}} \cong 0 \qquad C_{W\cdot S} = \frac{C_W C_v}{K_{DW}} \qquad (4.1.1\text{-}14)$$

$C_T = C_v + C_{A\cdot S} + C_{M\cdot S} + C_{E\cdot S} + C_{W\cdot S}$ -Total site equation (4.1.1-15)

From (4.1.1-8)

$$-r_S = k_S\left(C_{A\cdot S}C_{M\cdot S} - \frac{C_{E\cdot S}C_{W\cdot S}}{K_S}\right) \quad ; \quad K_S = \frac{k_S}{k_{-S}}$$

Substitute (4.1.1-11) to (4.1.1-14) into (4.1.1-15)

$$-r_S = k_S\left(K_{AB}C_A C_v K_{AM} C_M C_v - \frac{\frac{C_E C_v C_W C_v}{K_{DB}\,K_{DW}}}{K_S}\right)$$

$$-r_S = k_S K_{AB} K_{AM}\left(C_A C_M - \frac{C_E C_W}{K_{DB}K_{DW}K_S K_{AB}K_{AM}}\right)C_v^2 \qquad (4.1.1\text{-}16)$$

From (4.1.1.15) the vacant site equation can be expressed as seen below:

$$C_v = \frac{C_T}{1+K_{AB}C_A+K_{AM}C_M+\frac{C_E}{K_{DB}}+\frac{C_W}{K_{DW}}} \qquad (4.1.1\text{-}17)$$

Substitute (4.1.1-16) into (4.1.1-17)

$$-r_S = k_S K_{AB} K_{AM}\left(C_A C_M - \frac{C_E C_W}{K_S K_{AB}K_{AM}K_{DB}K_{DW}}\right)\left(\frac{C_T}{1+K_{AB}C_A+K_{AM}C_M+\frac{C_E}{K_{DB}}+\frac{C_W}{K_{DW}}}\right)^2$$

$$-r_S = \frac{K_1 K_{AB}K_{AM}\left(C_A C_M - \frac{C_E C_W}{K_S K_{AB}K_{AM}K_{DB}K_{DW}}\right)}{\left(1+K_{AB}C_A+K_{AM}C_M+\frac{C_E}{K_{DB}}+\frac{C_W}{K_{DW}}\right)^2} \qquad (4.1.1\text{-}18)$$

Table 2: Stoichiometric table for a Batch system

Species	Symbol	Initially	Change	Remaining	Concentration
$C_{15}H_{31}COOH$	A	N_{A_0}	$-N_{A_0}X$	$N_{A_0}(1-X)$	$C_{A_0}(1-X)$
CH_3OH	M	N_{M_0}	$-N_{A_0}X$	$N_{A_0}(\theta_M - X)$	$C_{A_0}(\theta_M - X)$

$C_{15}H_{31}OOCH_3$	E	N_{E_0}	$N_{A_0}X$	$N_{A_0}(\theta_E + X)$	$C_{A_0}(\theta_E + X)$
H_2O	W	N_{W_0}	$N_{A_0}X$	$N_{A_0}(\theta_W + X)$	$C_{A_0}(\theta_W + X)$

This is liquid-phase reaction; the density ρ is considered to be constant; therefore, $V = V_0$

$$C_A = \frac{N_A}{V} = \frac{N_A}{V_0} = \frac{N_{A_0}(1-X)}{V_0} = C_{A_0}(1-X)$$

$$\theta_M = \frac{C_{M_0}}{C_{A_0}} \qquad \theta_E = \frac{C_{E_0}}{C_{A_0}} \qquad \theta_W = \frac{C_{W_0}}{C_{A_0}}$$

$$\theta_M = \frac{C_{M_0}}{C_{A_0}} = \frac{1}{0.01} = 100$$

$$C_A = C_{A_0}(1-X) \qquad (4.1.1\text{-}19)$$

$$C_M = C_{A_0}(100-X) \qquad (4.1.1\text{-}20)$$

$$C_E = C_{A_0}X \qquad (4.1.1\text{-}21)$$

$$C_W = C_{A_0}X \qquad (4.1.1\text{-}22)$$

While $C_{A_0} = 0.246863\ \frac{mol}{dm^3}$

Substitute (4.1.1-19) to (4.1.1-22) into (4.1.1-18)

Therefore, the rate equation for the reaction limited is expressed as seen below:

$$rate = \frac{K_1\left(K_{AB}K_{AM}C_{A_0}(1-X)(100-X) - \frac{C_{A_0}X*X}{K_S K_{DB} K_{DW}}\right)}{\left(1+K_{AB}C_{A_0}(1-X)+K_{AM}C_{A_0}(100-X)+\frac{C_{A_0}X}{K_{DB}}+\frac{C_{A_0}X}{K_{DW}}\right)^2} \qquad (4.1.1\text{-}23)$$

II. Adsorption of palmitic acid is the rate-determining step. The k_{AM}, k_S, k_{DB}, k_{DW} are large by comparison, and we can set.

$$-\frac{r_{AM}}{k_{AM}} \cong 0 \qquad C_{M\cdot S} = K_{AM}C_M C_v \qquad (4.1.1\text{-}12)$$

$$-\frac{r_S}{k_S} \cong 0 \qquad C_{A\cdot S} = \frac{C_{E\cdot S}C_{W\cdot S}}{K_S C_{M\cdot S}} \qquad (4.1.1\text{-}24)$$

$$-\frac{r_{DB}}{k_{DB}} \cong 0 \qquad C_{E\cdot S} = \frac{C_E C_v}{K_{DB}} \qquad (4.1.1\text{-}13)$$

$$-\frac{r_{DW}}{k_{DW}} \cong 0 \qquad C_{W\cdot S} = \frac{C_W C_v}{K_{DW}} \qquad (4.1.1\text{-}14)$$

From (4.1.1-6)

$$-r_{AB} = -r_C = k_{AB}\left(C_A C_v - \frac{C_{A\cdot S}}{K_{AB}}\right)$$

Substitute (4.1.1-11) to (4.1.1-13) and (4.1.1-24) into (4.1.1-6) to obtain

$$-r_{AB} = k_{AB}\left(C_A C_v - \frac{\frac{C_{E\cdot S}C_{W\cdot S}}{K_S C_{M\cdot S}}}{K_{AB}}\right)$$

$$-r_{AB} = k_{AB}\left(C_A C_v - \frac{\frac{C_E C_v}{K_{DB}}\frac{C_W C_v}{K_{DW}}}{K_S K_{AM} C_M C_v}{K_{AB}}\right)$$

$$-r_{AB} = k_{AB}\left(C_A C_v - \frac{C_E C_W C_v}{K_{DB}K_{AB}K_{DW}K_S K_{AM}C_M}\right)$$

$$-r_{AB} = k_{AB}\left(C_A - \frac{C_E C_W}{K_{DB}K_{AB}K_{DW}K_S K_{AM}C_M}\right)C_v \qquad (4.1.1\text{-}25)$$

From (4.1.1-15) we can derive the vacant site equation as seen below:

$$C_v = \frac{C_T}{1+\frac{C_E C_W}{K_S K_{AM}K_{DB}K_{DW}C_M}+K_{AM}C_M+\frac{C_E}{K_{DB}}+\frac{C_W}{K_{DW}}} \qquad (4.1.1\text{-}26)$$

Substitute (4.1.1-26) into (4.1.1-25)

$$-r_{AB} = \frac{K_1\left(C_A-\frac{C_E C_W}{K_{DB}K_{AB}K_{DW}K_S K_{AM}C_M}\right)}{1+\frac{C_E C_W}{K_S K_{AM}K_{DB}K_{DW}C_M}+K_{AM}C_M+\frac{C_E}{K_{DB}}+\frac{C_W}{K_{DW}}} \qquad (4.1.1\text{-}27)$$

Substitute (4.1.1-19) to (4.1.1-22) into (4.1.1-27)

$$rate = \frac{K_1\left(C_{A_0}(1-X) - \frac{C_{A_0}X^2}{K_{DB}K_{AB}K_{DW}K_S K_{AM}(100-X)}\right)}{1+\frac{C_{A_0}X^2}{(100-X)K_{DB}K_{DW}K_S K_{AM}} + K_{AM}C_{A_0}(100-X) + \frac{C_{A_0}X}{K_{DB}} + \frac{C_{A_0}X}{K_{DW}}} \qquad (4.1.1\text{-}28)$$

III. Adsorption of methanol is the rate-determining step. The k_{AB}, k_S, k_{DB}, k_{DW} are large by comparison, and we can set.

$$-\frac{r_{AB}}{k_{AB}} \cong 0 \qquad C_{A\cdot S} = K_{AB}C_A C_v \qquad (4.1.1\text{-}11)$$

$$-\frac{r_S}{k_S} \cong 0 \qquad \frac{C_{W\cdot S}C_{E\cdot S}}{K_S C_{A\cdot S}} = C_{M\cdot S} \qquad (4.1.1\text{-}24)$$

$$-\frac{r_{DB}}{k_{DB}} \cong 0 \qquad C_{E\cdot S} = \frac{C_E C_v}{K_{DB}} \qquad (4.1.1\text{-}13)$$

$$-\frac{r_{DW}}{k_{DW}} \cong 0 \qquad C_{W\cdot S} = \frac{C_W C_v}{K_{DW}} \qquad (4.1.1\text{-}14)$$

From (4.1.1-7)

$$-r_{AM} = k_{AM}\left(C_M C_v - \frac{C_{M\cdot S}}{K_{AM}}\right)$$

Substitute (4.1.1-11), (4.1.1-24), (4.1.1-13) and (4.1.1-14) into (4.1.1-7) to obtain

$$-r_{AM} = k_{AM}\left(C_M C_v - \frac{\frac{C_{W\cdot S}C_{E\cdot S}}{K_S C_{A\cdot S}}}{K_{AM}}\right)$$

$$-r_{AM} = k_{AM}\left(C_M C_v - \frac{\frac{C_W C_v C_E C_v}{K_{DW}\,K_{DB}}}{\frac{K_S K_{AB} C_A C_v}{K_{AM}}}\right)$$

$$-r_{AM} = k_{AM}\left(C_M - \frac{C_W C_E}{K_S K_{AM} K_{AB} K_{DW} K_{DB} C_A}\right)C_v \qquad (4.1.1\text{-}29)$$

From (4.1.1-15)

$$C_v = \frac{C_T}{1+K_{AB}C_A + \frac{C_W C_E}{K_S K_{AB} K_{DW} K_{DB} C_A} + \frac{C_E}{K_{DB}} + \frac{C_W}{K_{DW}}} \qquad (4.1.1\text{-}30)$$

Substitute (4.1.1-30) into (4.1.1-29)

$$-r_{AM} = \frac{K_1\left(C_M - \frac{C_W C_E}{K_S K_{AM} K_{AB} K_{DW} K_{DB} C_A}\right)}{1 + K_{AB} C_A + \frac{C_W C_E}{K_S K_{AB} K_{DW} K_{DB} C_A} + \frac{C_E}{K_{DB}} + \frac{C_W}{K_{DW}}} \qquad (4.1.1\text{-}31)$$

Substitute (4.1.1-19) to (4.1.1-22) into (4.1.1-31)

$$rate = \frac{K_1\left(C_{A_0}(100 - X) - \frac{C_{A_0} X^2}{K_S K_{AM} K_{AB} K_{DW} K_{DB}(1-X)}\right)}{1 + K_{AB} C_{A_0}(1-X) + \frac{C_{A_0} X^2}{K_{DW} K_{DB} K_S K_{AB}(1-X)} + \frac{C_{A_0} X}{K_{DB}} + \frac{C_{A_0} X}{K_{DW}}} \qquad (4.1.1\text{-}32)$$

IV. Desorption of palmetate is a rate-determining step. The k_{AB}, k_{AM}, k_S, k_{DW} are large by comparison, and we can set.

$$-\frac{r_{AB}}{k_{AB}} \cong 0 \qquad C_{A\cdot S} = K_{AB} C_A C_v \qquad (4.1.1\text{-}11)$$

$$-\frac{r_{AM}}{k_{AM}} \cong 0 \qquad C_{M\cdot S} = K_{AM} C_M C_v \qquad (4.1.1\text{-}12)$$

$$-\frac{r_S}{k_S} \cong 0 \qquad C_{E\cdot S} = \frac{K_S C_{A\cdot S} C_{M\cdot S}}{C_{W\cdot S}} \qquad (4.1.1\text{-}24)$$

$$-\frac{r_{DW}}{k_{DW}} \cong 0 \qquad C_{W\cdot S} = \frac{C_W C_v}{K_{DW}} \qquad (4.1.1\text{-}14)$$

From (4.1.1-9)

$$-r_{DB} = k_{DB}\left(C_{E\cdot S} - \frac{C_E C_v}{K_{DB}}\right)$$

Substitute (4.1.1-11), (4.1.1-12), (4.1.1-14) and (4.1.1-24) into (4.1.1-9) to obtain

$$-r_{DB} = k_{DB}\left(C_{E\cdot S} - \frac{C_E C_v}{K_{DB}}\right)$$

$$-r_{DB} = k_{DB}\left(\frac{K_S C_{A\cdot S} C_{M\cdot S}}{C_{W\cdot S}} - \frac{C_E C_v}{K_{DB}}\right)$$

$$-r_{DB} = k_{DB}\left(\frac{K_S K_{AB} C_A C_v K_{AM} C_M C_v}{\frac{C_W C_v}{K_{DW}}} - \frac{C_E C_v}{K_{DB}}\right)$$

$$-r_{DB} = k_{DB}\left(\frac{K_S K_{AB} K_{AM} K_{DW} C_M C_A}{C_W} - \frac{C_E}{K_{DB}}\right) C_v \qquad (4.1.1\text{-}33)$$

From (4.1.1-15)

$$C_v = 1 + K_{AB}C_A + K_{AM}C_M + \frac{K_S K_{AB} K_{AM} K_{DW} C_A C_M}{C_W} + \frac{C_W}{K_{DW}} \quad (4.1.1\text{-}34)$$

Substitute (4.1.1-33) into (4.1.1-34)

$$-r_{DB} = \frac{K_1\left(\frac{K_S K_{AB} K_{AM} K_{DW} C_M C_A}{C_W} - \frac{C_E}{K_{DB}}\right)}{1 + K_{AB}C_A + K_{AM}C_M + \frac{K_S K_{AB} K_{AM} K_{DW} C_A C_M}{C_W} + \frac{C_W}{K_{DW}}} \quad (4.1.1\text{-}35)$$

Substitute (4.1.1-19) to (4.1.1-22) into (4.1.1-35) and simplify to obtain

$$rate = \frac{K_1\left(K_S K_{AB} K_{AM} K_{DW} C_{A_0}(100-X)(1-X) - \frac{C_{A_0} X^2}{K_{DB}}\right)}{X + K_{AB} C_{A_0} X(1-X) + K_{AM} C_{A_0} X(100-X) + K_S K_{AB} K_{AM} K_{DW} C_{A_0}(1-X)(100-X) + \frac{C_{A_0} X^2}{K_{DW}}} \quad (4.1.1\text{-}36)$$

V. Desorption of water is the rate-determining step. The k_{AB}, k_{AM}, k_S, k_{DB} are large by comparison, and we can set.

$$-\frac{r_{AB}}{k_{AB}} \cong 0 \qquad C_{A\cdot S} = K_{AB} C_A C_v \quad (4.1.1\text{-}11)$$

$$-\frac{r_{AM}}{k_{AM}} \cong 0 \qquad C_{M\cdot S} = K_{AM} C_M C_v \quad (4.1.1\text{-}12)$$

$$-\frac{r_S}{k_S} \cong 0 \qquad C_{W\cdot S} = \frac{K_S C_{A\cdot S} C_{M\cdot S}}{C_{E\cdot S}} \quad (4.1.1\text{-}13)$$

$$-\frac{r_{DB}}{k_{DB}} \cong 0 \qquad C_{E\cdot S} = \frac{C_E C_v}{K_{DB}} \quad (4.1.1\text{-}14)$$

From (4.1.1-10)

$$-r_{DW} = k_{DW}\left(C_{W\cdot S} - \frac{C_W C_v}{K_{DW}}\right)$$

$$-r_{DW} = k_{DW}\left(C_{W\cdot S} - \frac{C_W C_v}{K_{DW}}\right)$$

$$-r_{DW} = k_{DW}\left(\frac{K_S C_{A\cdot S} C_{M\cdot S}}{C_{E\cdot S}} - \frac{C_W C_v}{K_{DW}}\right)$$

$$-r_{DW} = k_{DW}\left(\frac{K_S K_{AB} C_A C_v K_{AM} C_M C_v}{\frac{C_E C_v}{K_{DB}}} - \frac{C_W C_v}{K_{DW}}\right)$$

$$-r_{DW} = k_{DW}\left(\frac{K_S K_{AB} K_{DB} K_{AM} C_A C_M}{C_E} - \frac{C_W}{K_{DW}}\right) C_v \quad (4.1.1\text{-}37)$$

From (4.1.1-15)

$$C_v = \frac{C_T}{1+K_{AB}C_A+K_{AM}C_M+\frac{C_E}{K_{DB}}+\frac{K_S K_{AB} K_{AM} K_{DB} C_M C_A}{C_E}} \quad (4.1.1\text{-}38)$$

Substitute (4.1.1-38) to (4.1.1-37)

$$-r_{DW} = \frac{K_1\left(\frac{K_S K_{AB} K_{DB} K_{AM} C_A C_M}{C_E} - \frac{C_W}{K_{DW}}\right)}{1+K_{AB}C_A+K_{AM}C_M+\frac{C_E}{K_{DB}}+\frac{K_S K_{AB} K_{AM} K_{DB} C_M C_A}{C_E}} \quad (4.1.1\text{-}39)$$

Substitute (4.1.1-19) to (4.1.1-22) into (4.1.1-39) and simplify to obtain

$$rate = \frac{K_1\left(K_S K_{AB} K_{DB} K_{AM} C_{A_0}(1-X)(100-X) - \frac{C_{A_0}X^2}{K_{DW}}\right)}{X+K_{AB}C_{A_0}X(1-X)+K_{AM}C_{A_0}X^2+\frac{C_{A_0}X^2}{K_{DB}}+K_S K_{AB} K_{AM} K_{DB} C_{A_0}(100-X)(1-X)} \quad (40)$$

4.1.2 Eley-Rideal model

In this model, the mechanism is for the reaction between an adsorbed molecule and a molecule in the fluid phase. There are two major models in this work. The first model assumes that palmitic acid is an adsorbed molecule. The second model assumes that methanol is an adsorbed molecule.

4.1.2.1 Palmitic acid is an adsorbed molecule

$A + S \overset{k_{AB}, k_{-AB}}{\Longleftrightarrow} A \cdot S$ -Adsorption of palmitic acid (4.1.2-1)

$A \cdot S + M \overset{k_S, k_{-S}}{\Longleftrightarrow} E \cdot S + W$ -Reaction of adsorbed palmitic acid with methanol (4.1.2-2)

$E \cdot S \overset{k_{DB} k_{-DB}}{\Longleftrightarrow} E + S$ -Desorption of ester (4.1.2-3)

$-r_{AB} = k_{AB}\left(C_A C_v - \left(\frac{C_{A\cdot S}}{K_{AB}}\right)\right); K_{AB} = \frac{k_{AB}}{k_{-AB}}$ -Rate of adsorption of palmitic acid (4.1.2-4)

$-r_S = k_S\left(C_{A\cdot S}C_M - \left(\frac{C_{E\cdot S}C_W}{K_S}\right)\right); K_S = \frac{k_S}{k_{-S}}$ -Rate of reaction of adsorbed palmitic acid with methanol (4.1.2-5)

$-r_{DB} = k_{DB}\left(C_{E\cdot S} - \left(\frac{C_E C_v}{K_{DB}}\right)\right); K_{DB} = \frac{k_{DB}}{k_{-DB}}$ -Rate of desorption of ester (4.1.2-6)

$C_T = C_v + C_{A\cdot S} + C_{E\cdot S}$ -Total site equation (4.1.2-7)

I. Adsorption of palmitic acid is a rate-determining step. The k_S and k_{DB} are large by comparison, and we can set.

$-\frac{r_S}{k_S} \cong 0$ $C_{A\cdot S} = \frac{C_{E\cdot S}C_W}{K_S C_M}$ (4.1.2-8)

$-\frac{r_{DB}}{k_{DB}} \cong 0$ $C_{E\cdot S} = \frac{C_E C_v}{K_{DB}}$ (4.1.2-9)

From (4.1.2-4)

$-r_{AB} = k_{AB}\left(C_A C_v - \left(\frac{C_{A\cdot S}}{K_{AB}}\right)\right)$

Substitute (4.1.2-8) and (4.1.2-9) into (4.1.2-4)

$-r_{AB} = k_{AB}\left(C_A C_v - \left(\frac{C_{E\cdot S}C_W}{K_S C_M K_{AB}}\right)\right)$

$-r_{AB} = k_{AB}\left(C_A - \left(\frac{C_E C_W}{K_{DB}K_S C_M K_{AB}}\right)\right)C_v$ (4.1.2-10)

From (4.1.2-7)

$C_T = C_v + \frac{C_E C_W C_v}{K_{DB}K_S C_M} + \frac{C_E C_v}{K_{DB}}$

$C_v = \frac{C_T}{1+\frac{C_W C_E}{K_{DB}K_S C_M}+\frac{C_E}{K_{DB}}}$ (4.1.2-11)

Substitute (4.1.2-11) into (4.1.2-10)

$$-r_{AB} = \frac{K_1\left(C_A - \left(\frac{C_E C_W}{K_{DB} K_S C_M K_{AB}}\right)\right)}{1 + \frac{C_W C_E}{K_{DB} K_S C_M} + \frac{C_E}{K_{DB}}} \qquad (4.1.2\text{-}12)$$

Substitute (4.1.1-19) to (4.1.1-22) into (4.1.2-12)

$$rate = \frac{K_1\left(C_{A_0}(1-X) - \left(\frac{C_{A_0} X^2}{K_{DB} K_S K_{AB}(100-X)}\right)\right)}{1 + \frac{C_{A_0} X^2}{K_{DB} K_S (100-X)} + \frac{C_{A_0} X}{K_{DB}}} \qquad (4.1.2\text{-}13)$$

II. Reaction of methanol with palmitic acid is a rate-determining step. The k_{AB} and k_{DB} are large by comparison, and we can set.

$$-\frac{r_{AB}}{k_{AB}} \cong 0 \qquad C_{A\cdot S} = K_{AB} C_A C_v \qquad (4.1.2\text{-}14)$$

$$-\frac{r_{DB}}{k_{DB}} \cong 0 \qquad C_{E\cdot S} = \frac{C_E C_v}{K_{DB}} \qquad (4.1.2\text{-}9)$$

From (4.1.2-5)

$$-r_S = k_S\left(C_{A\cdot S} C_M - \left(\frac{C_{E\cdot S} C_W}{K_S}\right)\right)$$

Substitute (4.1.2-9) and (4.1.2-14) into (4.1.2-5)

$$-r_S = k_S\left(K_{AB} C_A C_M - \left(\frac{C_W C_E}{K_{DB} K_S}\right)\right) C_v \qquad (4.1.2\text{-}15)$$

From (4.1.2-7)

$$C_T = C_v + K_{AB} C_A C_v + \frac{C_E C_v}{K_{DB}}$$

$$C_v = \frac{C_T}{1 + K_{AB} C_A + \frac{C_E}{K_{DB}}} \qquad (4.1.2\text{-}16)$$

Substitute (4.1.2-16) into (4.1.2-15)

$$-r_S = \frac{K_1\left(K_{AB} C_A C_M - \left(\frac{C_W C_E}{K_{DB} K_S}\right)\right)}{1 + K_{AB} C_A + \frac{C_E}{K_{DB}}} \qquad (4.1.2\text{-}17)$$

Substitute (4.1.1-19) to (4.1.1-22) into (4.1.2-17)

$$-r_S = \frac{K_1\left(K_{AB}{C_{A_0}}^2(1-X)(100-X) - \left(\frac{{C_{A_0}}^2X^2}{K_{DB}K_S}\right)\right)}{1+K_{AB}C_{A_0}(1-X)+\frac{C_{A_0}X}{K_{DB}}} \qquad (4.1.2\text{-}18)$$

III. Desorption of ester is a rate-determining step. The k_{AB} and k_S are large by comparison, and we can set.

$$-\frac{r_{AB}}{k_{AB}} \cong 0 \qquad C_{A\cdot S} = K_{AB}C_AC_v \qquad (4.1.2\text{-}14)$$

$$-\frac{r_S}{k_S} \cong 0 \qquad C_{A\cdot S} = \frac{C_{E\cdot S}C_W}{K_SC_M};\ C_{E\cdot S} = \frac{K_SC_MC_{A\cdot S}}{C_W} \qquad (4.1.2\text{-}8)$$

From (4.1.2-6)

$$-r_{DB} = k_{DB}\left(C_{E\cdot S} - \left(\frac{C_EC_v}{K_{DB}}\right)\right)$$

$$-r_{DB} = k_{DB}\left(\frac{K_SC_MK_{AB}C_A}{C_W} - \left(\frac{C_E}{K_{DB}}\right)\right)C_v \qquad (4.1.2\text{-}19)$$

From (4.1.2-7)

$$C_T = C_v + K_{AB}C_AC_v + \frac{K_SK_{AB}C_MC_AC_v}{C_W}$$

$$C_v = \frac{C_T}{1+K_{AB}C_A+\frac{K_SK_{AB}C_MC_A}{C_W}} \qquad (4.1.2\text{-}20)$$

Substitute (4.1.2-19) into (4.1.2-20)

$$-r_{DB} = \frac{K_1\left(\frac{K_SK_{AB}C_MC_A}{C_W} - \left(\frac{C_E}{K_{DB}}\right)\right)}{1+K_{AB}C_A+\frac{K_SK_{AB}C_MC_A}{C_W}} \qquad (4.1.2\text{-}21)$$

Substitute (4.1.1-19) to (4.1.1-22) into (4.1.2-21)

$$-r_{DB} = \frac{K_1\left(\frac{K_{AB}K_SC_{A_0}(1-X)(100-X)}{X} - \left(\frac{C_{A_0}X}{K_{DB}}\right)\right)}{1+K_{AB}C_{A_0}(1-X)+\frac{K_SK_{AB}C_{A_0}(1-X)(100-X)}{X}} \qquad (4.1.2\text{-}22)$$

Simplify to obtain

$$rate = \frac{K_1\left(K_{AB}K_S C_{A_0}(1-X)(100-X) - \left(\frac{C_{A_0}X^2}{K_{DB}}\right)\right)}{X + K_{AB}C_{A_0}X(1-X) + K_S K_{AB} C_{A_0}(1-X)(100-X)} \quad (4.1.2\text{-}23)$$

4.1.2.2 Methanol is an adsorbed molecule

$M + S \overset{k_{AM}, k_{-AM}}{\Longleftrightarrow} MS$ -Adsorption of methanol (4.1.2-24)

$M \cdot S + A \overset{k_S, k_{-S}}{\Longleftrightarrow} W \cdot S + E$ -Reaction of adsorbed methanol with palmitic acid (4.1.2-25)

$W \cdot S \overset{k_{DW} k_{-DW}}{\Longleftrightarrow} W + S$ -Desorption of water (4.1.2-26)

$-r_{AM} = k_{AM}\left(C_M C_v - \frac{C_{M\cdot S}}{K_{AM}}\right); K_{AM} = \frac{k_{AM}}{k_{-AM}}$ -Rate of adsorption of methanol (4.1.2-27)

$-r_S = k_S\left(C_{M\cdot S} C_A - \frac{C_{W\cdot S} C_E}{K_S}\right); K_S = \frac{k_S}{k_{-S}}$ -Rate of reaction of adsorbed methanol with palmitic acid (4.1.2-28)

$-r_{DW} = k_{DW}\left(C_{W\cdot S} - \frac{C_W C_v}{K_{DW}}\right); K_{DW} = \frac{k_{DW}}{k_{-DW}}$ -Rate of desorption of water (4.1.2-29)

$C_T = C_v + C_{M\cdot S} + C_{W\cdot S}$ -Total site equation (4.1.2-30)

I. Adsorption of methanol is a rate-determining step. The k_S and k_{DW} are large by comparison, and we can set.

$-\frac{r_S}{k_S} \cong 0$ $C_{M\cdot S} = \frac{C_{W\cdot S} C_E}{K_S C_A}$ (4.1.2-31)

$-\frac{r_{DW}}{k_{DW}} \cong 0$ $C_{W\cdot S} = \frac{C_W C_v}{K_{DW}}$ (4.1.2-32)

From (4.1.2-27)

$$-r_{AM} = k_{AM}\left(C_M C_v - \frac{C_{M\cdot S}}{K_{AM}}\right)$$

Substitute (4.1.2-31) and (4.1.2-32) into (4.1.2-27)

$$-r_{AM} = k_{AM}\left(C_M - \frac{C_W C_E}{K_{DW}K_S K_{AM} C_A}\right)C_v \qquad (4.1.2\text{-}32)$$

From (4.1.2-30)

$$C_T = C_v + \frac{C_E C_W C_v}{K_{DW}K_S C_A} + \frac{C_W C_v}{K_{DW}}$$

$$C_v = \frac{C_T}{1+\frac{C_W C_E}{K_{DW}K_S C_A}+\frac{C_E}{K_{DW}}} \qquad (4.1.2\text{-}33)$$

Substitute (4.1.2-33) into (4.1.2-32)

$$-r_{AM} = \frac{K_1\left(C_M - \frac{C_W C_E}{K_{DW}K_S K_{AM} C_A}\right)}{1+\frac{C_W C_E}{K_{DW}K_S C_A}+\frac{C_E}{K_{DW}}} \qquad (4.1.2\text{-}34)$$

Substitute (4.1.1-19) to (4.1.1-22) into (4.1.2-34)

$$rate = \frac{K_1\left(C_{A_0}(100-X) - \frac{C_{A_0}X^2}{K_{DW}K_S K_{AM}}\right)}{1+\frac{C_{A_0}X^2}{K_{DW}K_{S(1-X)}}+\frac{C_{A_0}X}{K_{DW}}} \qquad (4.1.2\text{-}35)$$

II. Reaction is a rate-determining step. The k_{AM} and k_{DW} are large by comparison, and we can set.

$$-\frac{r_{AM}}{k_{AM}} \cong 0 \qquad C_{M\cdot S} = K_{AM} C_M C_v \qquad (4.1.2\text{-}36)$$

$$-\frac{r_{DW}}{k_{DW}} \cong 0 \qquad C_{W\cdot S} = \frac{C_W C_v}{K_{DW}} \qquad (4.1.2\text{-}32)$$

From (4.1.2-28)

$$-r_S = k_S\left(C_{M\cdot S} C_A - \frac{C_{W\cdot S} C_E}{K_S}\right)$$

$$-r_S = k_S\left(K_{AM} C_M C_A - \frac{C_E C_W}{K_{DW}K_S}\right)C_v \qquad (4.1.2\text{-}37)$$

From (4.1.2-30)

$$C_T = C_v + K_{AM}C_M C_v + \frac{C_W C_v}{K_{DW}}$$

$$C_v = \frac{C_T}{1+K_{AM}C_M+\frac{C_W}{K_{DW}}} \qquad (4.1.2\text{-}38)$$

Substitute (4.1.2-38) into (4.1.2-37)

$$-r_S = \frac{K_1\left(K_{AM}C_M C_A - \frac{C_E C_W}{K_{DW}K_S}\right)}{1+K_{AM}C_M+\frac{C_W}{K_{DW}}} \qquad (4.1.2\text{-}39)$$

Substitute (4.1.1-19) to (4.1.1-22) into (4.1.2-39)

$$rate = \frac{K_1\left(K_{AM}{C_{A_0}}^2(100-X)(1-X) - \frac{{C_{A_0}}^2X^2}{K_{DW}K_S}\right)}{1+K_{AM}C_{A_0}(100-X)+\frac{C_{A_0}X}{K_{DW}}} \qquad (4.1.2\text{-}40)$$

III. Desorption of water is a rate-determining step. The k_{AM} and k_S are large by comparison, and we can set

$$-\frac{r_{AM}}{k_{AM}} \cong 0 \qquad C_{M\cdot S} = K_{AM}C_M C_v \qquad (4.1.2\text{-}36)$$

$$-\frac{r_S}{k_S} \cong 0 \qquad C_{M\cdot S} = \frac{C_{W\cdot S}C_E}{K_S C_A}\,;\, C_{W\cdot S} = \frac{K_S C_A C_{M\cdot S}}{C_E} \qquad (4.1.2\text{-}31)$$

From (4.1.2-29)

$$-r_{DW} = k_{DW}\left(C_{W\cdot S} - \frac{C_W C_v}{K_{DW}}\right)$$

$$-r_{DW} = k_{DW}\left(\frac{K_{AM}K_S C_M C_A}{C_E} - \frac{C_W}{K_{DW}}\right)C_v \qquad (4.1.2\text{-}41)$$

From (4.1.2-38)

$$C_T = C_v + K_{AM}C_M C_v + \frac{K_{AM}K_S C_M C_A C_v}{C_E}$$

$$C_v = \frac{C_T}{1+K_{AM}C_M+\frac{K_{AM}K_S C_M C_A}{C_E}} \qquad (4.1.2\text{-}42)$$

Substitute (4.1.2-42) into (4.1.2-41)

$$-r_{DW} = \frac{K_1\left(\frac{K_{AM}K_S C_M C_A}{C_E} - \frac{C_W}{K_{DW}}\right)}{1+K_{AM}C_M+\frac{K_{AM}K_S C_M C_A}{C_E}} \quad (4.1.2\text{-}43)$$

Substitute (4.1.1-19) to (4.1.1-22) into (4.1.2-43)

$$-r_{DW} = \frac{K_1\left(\frac{K_S K_{AM} C_{A_0}(100-X)(1-X)}{X} - \frac{C_{A_0}X}{K_{DW}}\right)}{1+K_{AM}C_{A_0}(100-X)+\frac{K_S K_{AM} C_{A_0}(100-X)(1-X)}{X}} \quad (4.1.2\text{-}44)$$

Multiply $\frac{X}{X}$ to (4.1.2-44)

$$-r_{DW} = \frac{K_1\left(K_S K_{AM} C_{A_0}(100-X)(1-X) - \frac{C_{A_0}X^2}{K_{DW}}\right)}{X+K_{AM}C_{A_0}X(100-X)+K_S K_{AM} C_{A_0}(100-X)(1-X)} \quad (4.1.2\text{-}45)$$

4.2 Model for reactor

In the experiment, the batch reactor was used. The equation of the batch reactor was derived (Fogler,2006) as

$$\frac{dN_A}{dt} = \int^V r_A dV \quad (4.2\text{-}1)$$

Assume that the reaction mixture is perfectly mixed so that there is no variation in the rate of reaction throughout the reactor volume. Therefore, we can take r_A out of the integral. The reaction is also in the liquid phase, and the volume is constant. Therefore, the eq. (4.2-1) can be transformed into the following equation:

$$\frac{dN_A}{dt} = r_A V \quad (4.2\text{-}2)$$

Divided by V

$$\frac{dC_A}{dt} = r_A \quad (4.2\text{-}3)$$

From (4.1.1-19)

$$C_A = C_{A_0}(1-X)$$

The (4.2-3) can be transformed into

$$C_A \frac{dX}{dt} = -r_A \qquad (4.2\text{-}4)$$

We substituted the entire rate law model into (4.2-4). Then, we tested the models with the reaction rates from the experiment.

4.3 SO_4/ZrO_2-550°C kinetic mechanisms

After testing all the models, the Eley-Rideal mechanism, which assumed that the surface reaction between adsorbed palmetic acid and methanol in the bulk fluid was the rate-determining step, was fitted to the experimental data. The mechanism consisted of three elementary reactions as described below:

$$A + S \overset{K_{AB}}{\Longleftrightarrow} AS$$

$$AS + M \overset{K_S}{\Leftrightarrow} ES + W$$

$$ES \overset{K_{DB}}{\Longleftrightarrow} E + S$$

Here, A is palmitic acid, S is an active site on the surface, M is methanol, W is water, E is palmitic methyl ester, and AS and ES are adsorbed intermediates. The kinetic model was built based on following assumptions:

1. The surface reaction was the rate-determining step.
2. The adsorption and desorption of reactants and products are fast and at equilibrium.
3. The rate of the non-catalyzed reactions compared to the catalyzed reactions can be neglected.

4. The diffusion rate of the product and reactant from the catalyst surface is fast and can be neglected.
5. There are no differences in the activity and accessibility of sites on the catalyst surface.
6. There are no palmitic methyl ester and water before the reaction.

Based on the assumptions above, the following kinetic rate law is derived:

$$rate = \frac{K_1\left(K_{AB}C_AC_M - \left(\frac{C_WC_E}{K_{DB}K_S}\right)\right)}{1+K_{AB}C_A+\frac{C_E}{K_{DB}}} \qquad (4.1.2\text{-}17)$$

Here, K_S, K_{AB}, and K_D represent the equilibrium constants of the surface reaction, adsorption of palmitic acid, and desorption of palmitic methyl ester respectively. In the equation $K_1 = C_T k_s$, k_s is the forward reaction rate constant.

The concentration of the reactants and products can be expressed as

$$C_A = C_{A_0}(1 - X)$$

$$C_M = C_{A_0}(100 - X)$$

$$C_E = C_{A_0}X$$

$$C_W = C_{A_0}X$$

Therefore, the equation can be expressed as:

$$rate = \frac{K_1\left(K_{AB}{C_{A_0}}^2(1-X)(100-X)-\left(\frac{{C_{A_0}}^2X^2}{K_{DB}K_S}\right)\right)}{1+K_{AB}C_{A_0}(1-X)+\frac{C_{A_0}X}{K_{DB}}} \qquad (4.1.2\text{-}18)$$

The result of this model against experimental data is shown in Figure 5.

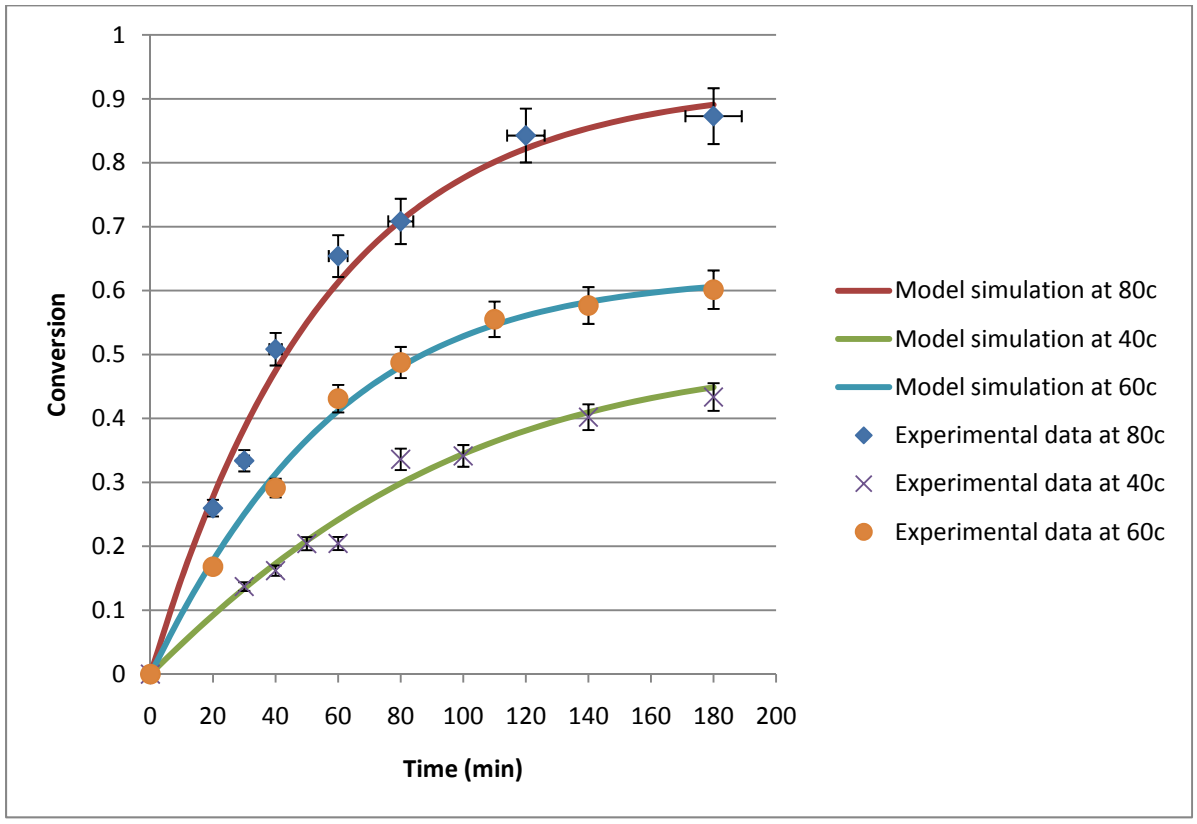

Figure 5: Fitting of Eley-Rideal model to experimental data for palmitic acid esterification over SO_4/ZrO_2-550°C at 40, 60 and 80oC

The coefficients of determination of the deterministic model were 0.98, 0.99, and 0.99 for SO_4/ZrO_2-550°C at 40, 60, and 80°C. Therefore, the esterification of palmitic acid over SO_4/ZrO_2-550°C obeys the Eley-Rideal mechanism. The reaction of adsorbed palmitic acid with methanol in the bulk fluid is the rate-

determining step for SO_4/ZrO_2-550°C. The kinetic parameter is shown in Table 3.

Table 3: Kinetic parameters of palmitic acid esterification on SO_4/ZrO_2-550°C

Temp(C)	$K_1 \times 10^{-4}$	$K_{AB} \times 10^{-2}$	K_{DB}	$K_S \times 10^{-3}$
40	3.78	59.75	2.01	4.21
60	16.12	26.74	2.01	19.38
80	51.10	13.38	9.08	92.41

The esterification mechanisms of palmitic acid, which occurs over SO_4/ZrO_2-550°C, is shown in Figure 6.

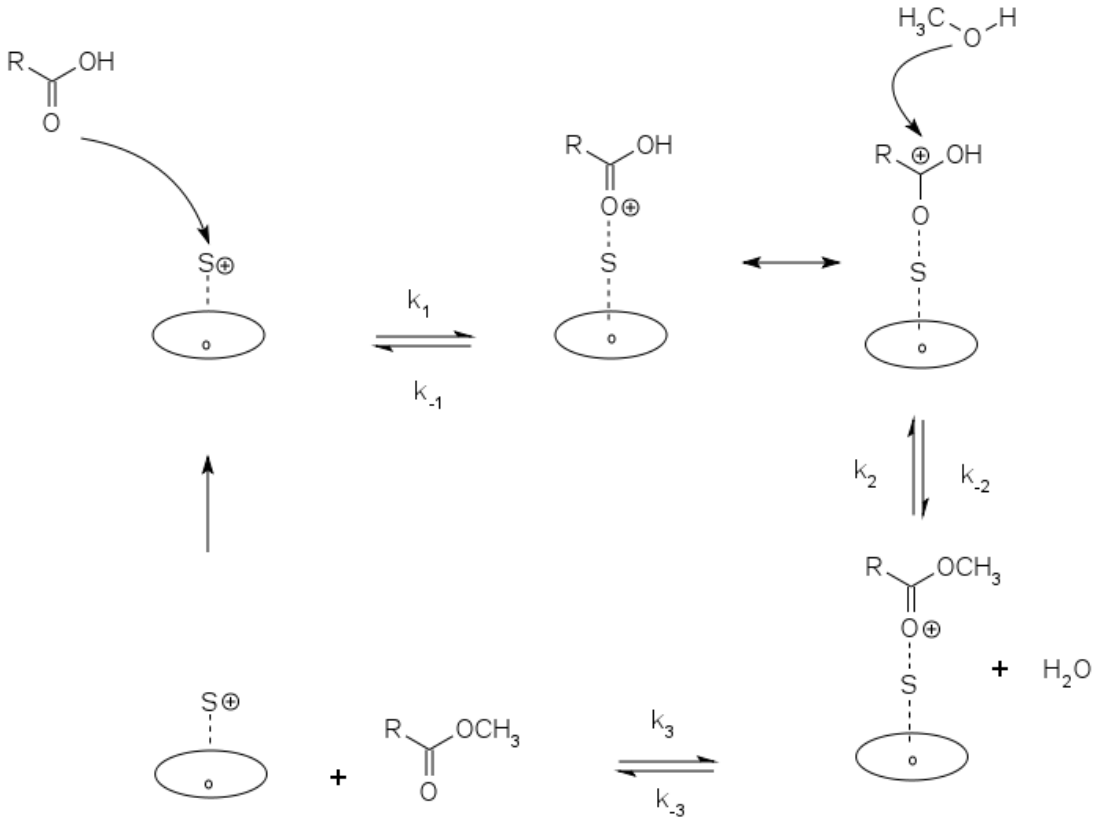

$S^{\oplus}$ = active acid site on catalyst

R = $CH_3(CH_2)_{14}$

Figure 6: Illustration of palmitic acid esterification over SO_4/ZrO_2-550°C

4.4 $AcAl_2O_3$ kinetic model

After testing all the models, the Eley-Rideal mechanism, which assumed that methanol adsorption on the surface was the rate-determining step for $AcAl_2O_3$, was fitted to the experimental data. The mechanisms consisted of three elementary reactions as described below:

$$M + S \overset{K_{AM}}{\Longleftrightarrow} MS$$

$$M \cdot S + A \overset{K_S}{\Leftrightarrow} W \cdot S + E$$

$$W \cdot S \overset{K_{DW}}{\Longleftrightarrow} W + S$$

where M is methanol, S is an active site, A is palmitic acid, W is water, E is palmitic acid methyl ester, and MS and WS are surface intermediates. The kinetic model was built based on similar assumptions as in SO_4/ZrO_2 The following kinetic rate law was derived:

$$rate = \frac{K_1\left(C_M - \frac{C_W C_E}{K_{DW} K_S K_{AM} C_A}\right)}{1 + \frac{C_W C_E}{K_{DW} K_S C_A} + \frac{C_E}{K_{DW}}} \qquad (4.1.2\text{-}34)$$

Here, K_S, K_{AM}, and K_D represent the equilibrium constants of the surface reaction, adsorption of palmitic acid, desorption of palmitic acid methyl ester respectively. In the equation $K_1 = C_T k_{AM}$, k_{AM} is the forward rate constant of adsorption of methanol.

The concentration of the reactants and products can be expressed as:

$$C_A = C_{A_0}(1 - X)$$

$$C_M = C_{A_0}(100 - X)$$

$$C_E = C_{A_0}X$$

$$C_W = C_{A_0}X$$

Therefore, the equation can be expressed as:

$$rate = \frac{K_1\left(C_{A_0}(100-X) - \frac{C_{A_0}X^2}{K_{DW}K_S K_{AM}}\right)}{1 + \frac{C_{A_0}X^2}{K_{DW}K_S(1-X)} + \frac{C_{A_0}X}{K_{DW}}} \qquad (4.1.2\text{-}35)$$

The result of this model against experimental data is shown in Figure 7.

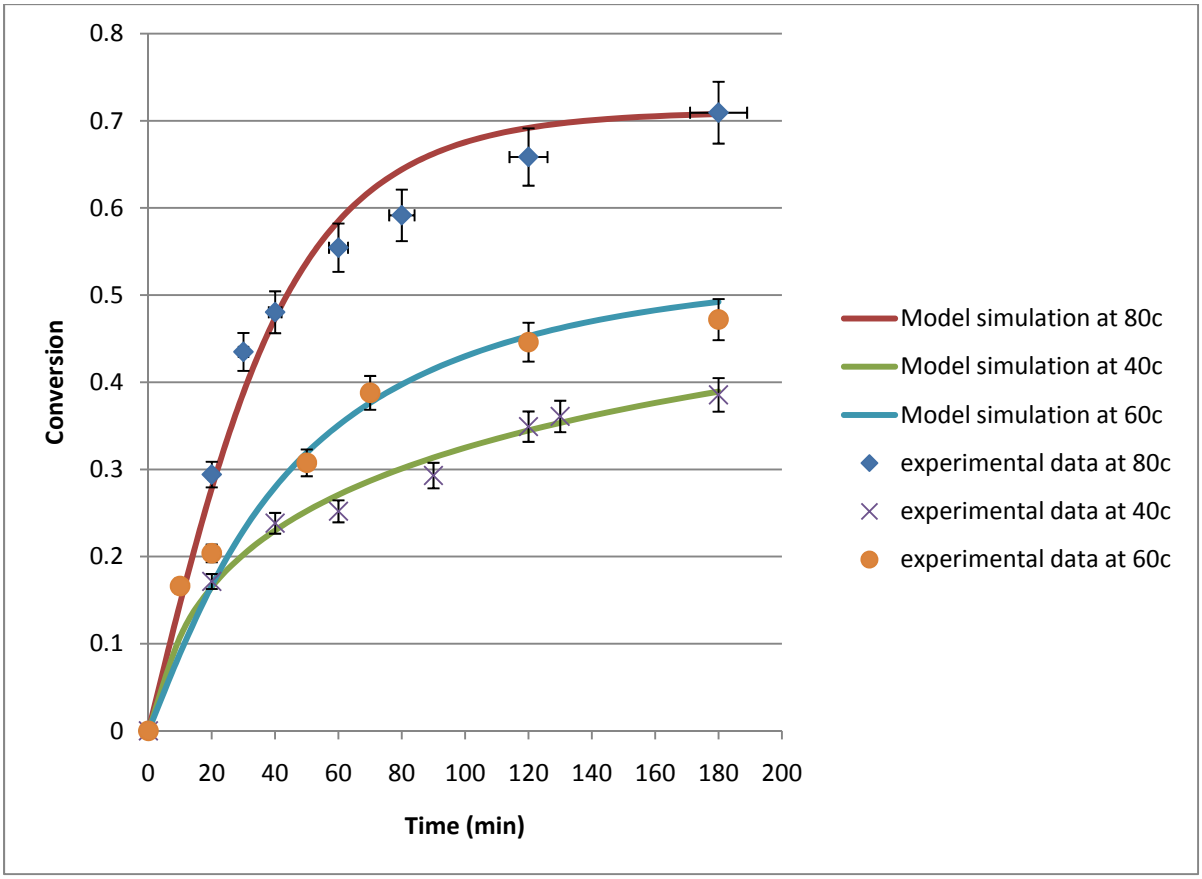

Figure 7: Fitting of Eley-Rideal model to experimental data for palmitic acid esterification over $AcAl_2O_3$ at 40, 60 and 80°C

The coefficients of determination of the deterministic model were 0.99, 0.98, and 0.96 for $AcAl_2O_3$ at 40, 60, and 80°C. Therefore, the esterification of palmitic acid with methanol on $AcAl_2O_3$ follows the Eley-Rideal mechanism. The adsorption of methanol on an active site on the catalyst was the rate-determining step in $AcAl_2O_3$. The kinetic parameters are shown in Table 4.

Table 4: Kinetic parameters of palmitic acid esterification on $AcAl_2O_3$

Temp(C)	$K_1 \times 10^{-4}$	K_{AM}	K_{DB}	$K_S \times 10^{-1}$
40	1.36	2.01	2.17	0.02
60	0.91	0.14	2.01	0.21
80	1.50	0.08	2.01	1.14

The esterification mechanisms of palmitic acid, catalyzed by $AcAl_2O_3$ is shown in Figure 8.

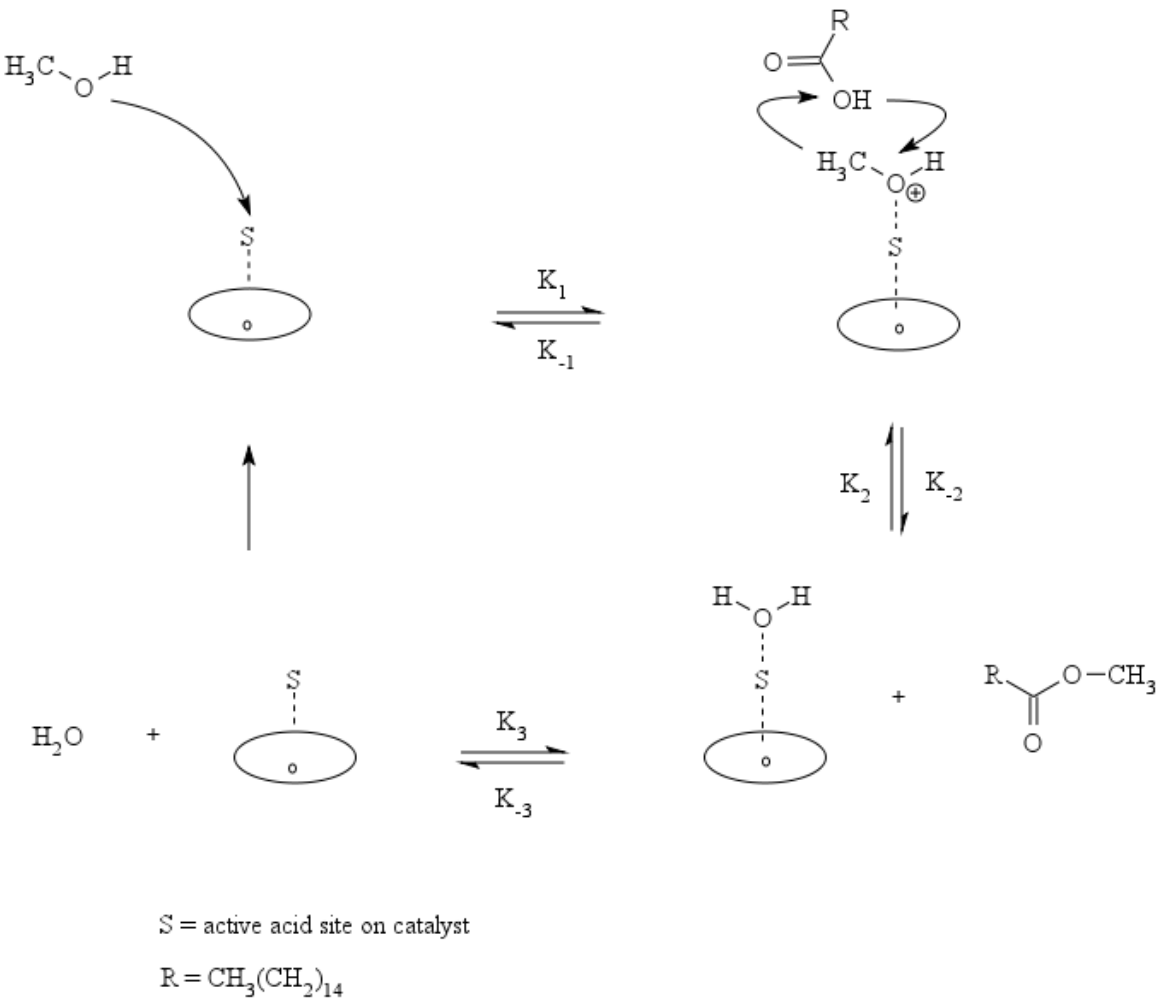

Figure 8: Illustration of palmitic acid esterification over $AcAl_2O_3$

4.5 Determined the heat of the reaction on both catalysts

To evaluate the efficiency of the catalysts, the activation energies were determined. The reaction rate constant is related to the reaction temperature through the Arrhenius equation. Therefore, the overall reaction heat of the reaction can be

calculated from equation below using the reaction rate constant K_S:

$$K_S = Aexp\left(-\frac{\Delta E}{RT}\right)$$

Both the frequency factor A and the heat of the reaction Ea were obtain by plotting $ln(K_S)$ against 1/T. The heat of the reaction of palmitic acid esterification was 70.81 kJ/mol and 93.71 KJ/mol for SO_4/ZrO_2-550°C and $AcAl_2O_3$ respectively.

4.6 Predicted conversion using the deterministic model

In order to validate the models, we used them to predict the percent conversion at 210 minutes and 240 minutes at all temperatures for all catalysts. We then compared the predicted values with actual experimental data.

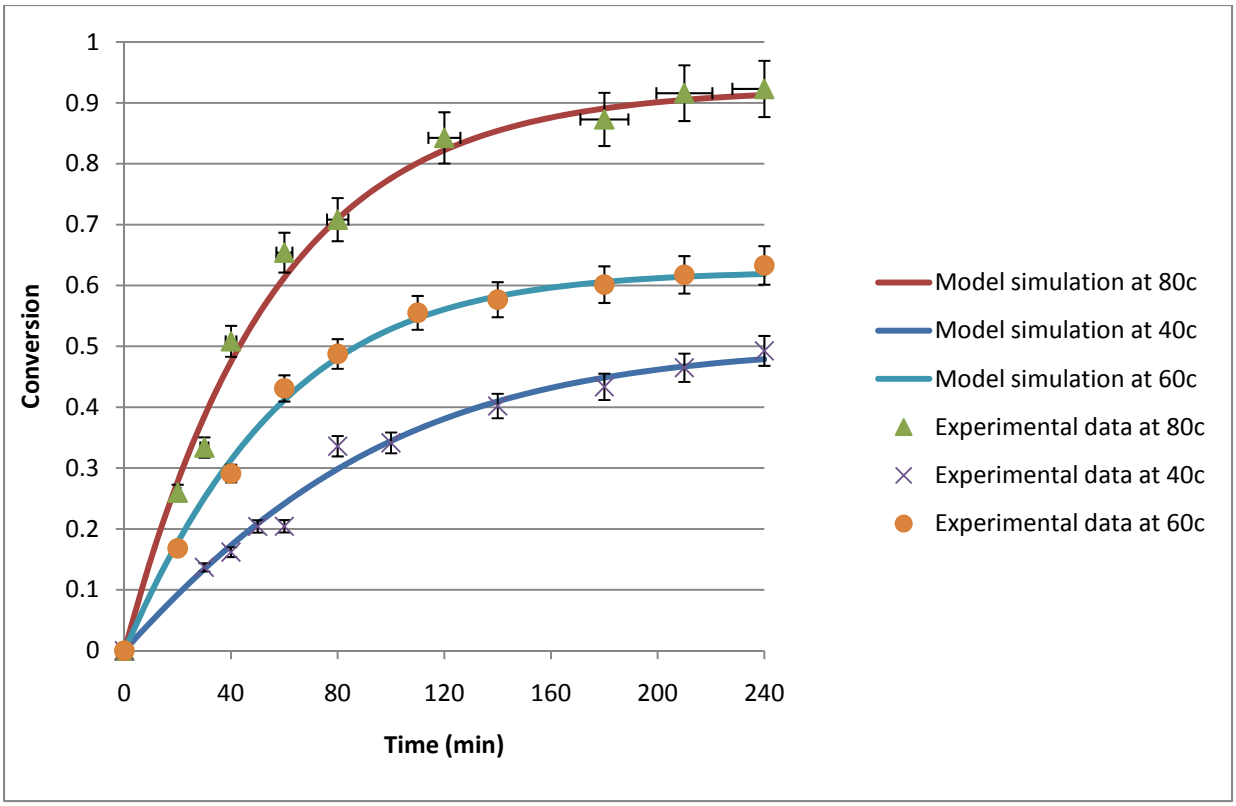

Figure 9: Prediction of Esterification of Palmitic Acid over Zirconia Sulfate

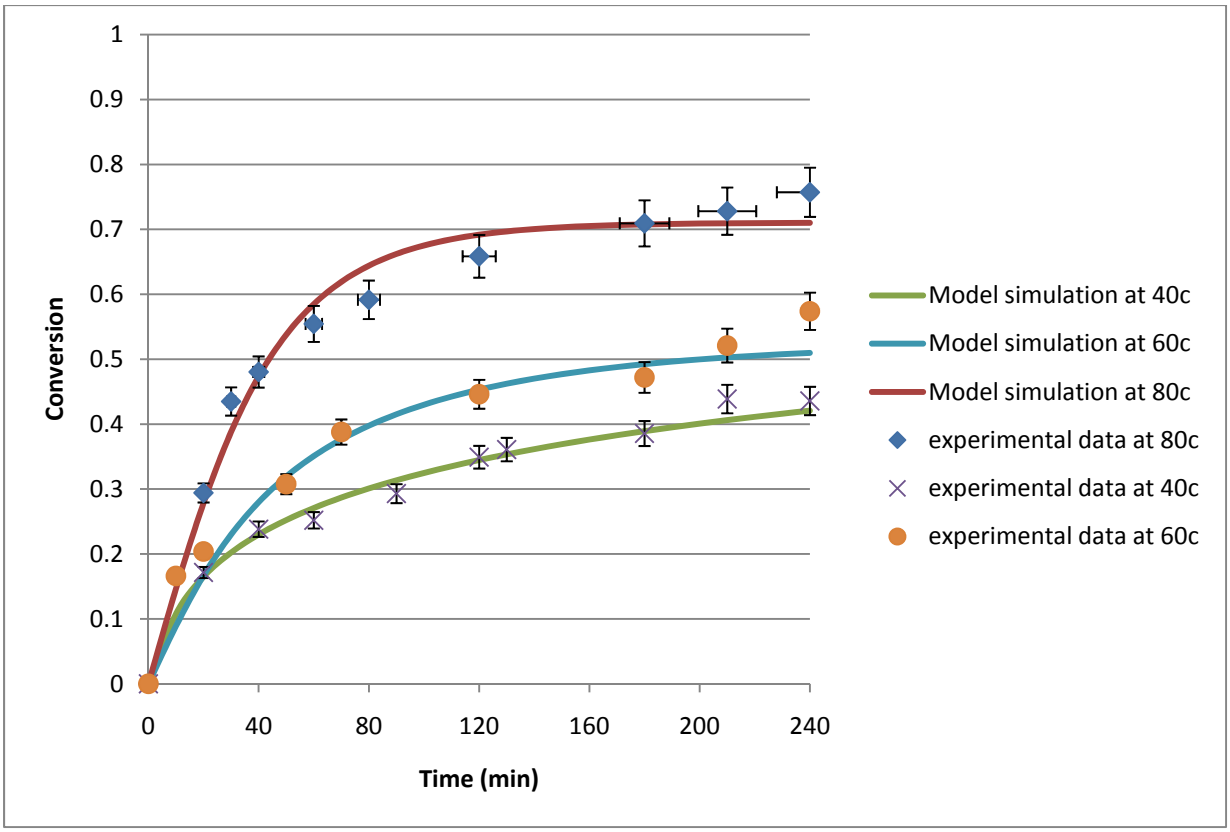

Figure 10: Prediction of Esterification of Palmitic Acid on Alumina

As can be seen in Figure 9 and Figure 10, the deterministic models used to predict the conversion at times greater than 180 minutes showed good agreement. The values of the deterministic models are very close to the experimental data. Therefore, these rate law models can be used to predict the experimental data at different temperatures between 40°C to 80°C and at longer reaction times.

4.7 Discussion

This disparity between the adsorbed species is attributed to the nature of the acidic sites on the catalysts. Sulfated zirconium oxide has been reported to have Brönsted and Lewis acid

sites. When the reaction was carried over pure zirconium oxide, the esterification yield was low; therefore, it was assumed that the catalyst activity was mostly due to the Brönsted acid sites generated by the sulfation. Activated acidic alumina, however, only has Lewis acid sites. The adsorption of palmitic acid is believed to be a nucleophilic interaction between the Brönsted acid site and the carboxylic moiety similar to homogeneous acid catalyzed esterification. On the activated acidic alumina, however, Lewis acid sites are predominant leading to the chemisoption of methanol. Therefore, Brönsted acid behaves differently from Lewis acid in the esterification of free fatty acid.

From the heat of the reaction of both catalysts, SO_4/ZrO_2-550°C seems to be a better catalyst in the esterification of palmitic acid. However, this catalyst requires sulfation and temperature activation before use. On the other hand, $AcAl_2O_3$ does not require sulfation, though three hours of activation at 550°C is required in order to remove moisture and atmospheric carbon from the surface. Therefore, it is more convenient for industrial use where easy-to-prepare catalysts are needed, although the operation cost of $AcAl_2O_3$ may be higher due to the higher heat of the reaction requiring higher temperature.

Chapter 5 Stochastic Simulation

Computer simulations can be vital in investigating a chemical reaction. The simulation can aid in the exploration of complex dynamics of reaction. There are two approaches in computer simulation, namely deterministic and stochastic (Mira, et al.,2003). The deterministic approach uses a set of differential equations to explain the time dependence of the concentrations in the chemical system.

In the stochastic approach, it is assumed that each reaction proceeds independently and randomly and can occur with a certain probability associated with the thermodynamic properties of the reacting molecules. The stochastic chemical kinetics describes interactions involving a discrete number of molecules. The stochastic algorithm is appropriate when the number of molecules in a system is small. In a given initial number of molecules, there are many possible time evolutions, each of which has their own probability. The summation of all the probabilities has to add up to one.

There is a link between deterministic and stochastic simulation. The reaction rate constants of the deterministic simulation can be interpreted in terms of probabilities in the stochastic simulation. The differential equations in the deterministic simulation are similar to the stochastic approach.

5.1 Stochastic approach

The nature of chemical reactions is stochastic (de Levie,2000). Each reaction is a discrete event that takes place with a given probability. An aspect of this simulation is that it can determine whether a proposed reaction mechanism is consistent with the observed result. The stochastic algorithm is as follows (Gillespie,2007):

1. $P_0(\tau|x,t)$ is the probability that no reaction will occur in the time interval $[t,t+\tau)$.
2. $p(\tau,j|x,t)d\tau$ is the probability that the next reaction will be j^{th}reaction and occur during the time interval $[t+\tau,t+\tau+d\tau)$.
3. X(t)=x is a number of molecules of any species.
4. $a_j(X(t))$ is a propensity function of j^{th}reaction.
5. ν_j is a state-change vector of j^{th}reaction.
6. c_j is a reaction rate constant of j^{th}reaction.

If the time of the reaction is very small, the assumption is that what happens over $[t,t+\tau)$ is independent of what happens over $[t+\tau,t+\tau+d\tau)$.

$$\begin{aligned} P_0(\tau+d\tau|x,t) &= P_0(\tau|x,t) \cup P_0(\tau|x,t+\tau)d\tau \\ &= P_0(\tau|x,t) \times P_0(\tau|x,t+\tau)d\tau \\ &= P_0(\tau|x,t) \times (1-\sum p(\tau,j|x,t)\,d\tau) \end{aligned}$$

From the definition of the propensity function

$$P_0(\tau+d\tau|x,t) = P_0(\tau|x,t)\left(1-\sum_{k=1}^{M} a_k(x)d\tau\right)$$

From the proof in (Higham,2008)

$$p(\tau,j|x,t) = \frac{a_j(x)}{a_{sum}(x)}\left(a_{sum}(x)e^{-a_{sum}(x)\tau}\right)$$

$\frac{a_j(x)}{a_{sum}(x)}$ is the next reaction index which corresponds to a discrete random variable that controls the chance of picking the j^{th} reaction while $a_{sum}(x)e^{-a_{sum}(x)\tau}$ is the time until the next reaction and is the density function for a continuous random variable with an exponential distribution.

Assuming good mixing and negligible surface diffusion, the resulting algorithm can be summarized in the following pseudo code:

1. Evaluate $\{a_k(X(t))\}_{k=1}^{M}$ and $a_{sum}(X(t)) \coloneqq \sum_{k=1}^{M} a_k(X(t))$.

2. Draw two independent uniform (0,1) random numbers, $\xi_1$and ξ_2

3. Set j to be the smallest integer satisfying $\sum_{k=1}^{j} a_k\big(X(t)\big) > \xi_1 a_{sum}(X(t))$.

4. Set $\tau = \frac{\ln(\frac{1}{\xi_2})}{a_{sum}(X(t))}$

5. Set $X(t+\tau) = X(t) + \nu_j$

6. Return to step 1

5.2 SO_4/ZrO_2-550°C stochastic simulation

There are six sub-chemical reactions that occur during the esterification of palmitic acid over SO_4/ZrO_2-550°C. The solution contains seven species and X_n represents the n^{th} species. The six sub-reactions are illustrated below:

1. $X_1 + X_2 \xrightarrow{C_1} X_3$ (1) $a_1 = C_1 X_1 X_2$

2. $X_3 \xrightarrow{C_2} X_1 + X_2$ (2) $a_2 = C_2 X_2$

3. $X_3 + X_4 \xrightarrow{C_3} X_5 + X_6$ (3) $a_3 = C_3 X_3 X_4$

4. $X_5 + X_6 \xrightarrow{C_4} X_3 + X_4$ (4) $a_4 = C_4 X_5 X_6$

5. $X_5 \xrightarrow{C_5} X_7 + X_2$ (5) $a_5 = C_5 X_5$

6. $X_2 + X_7 \xrightarrow{C_6} X_5$ (6) $a_6 = C_6 X_2 X_7$

Here,

- X_1 is palmitic acid

- X_2 is a vacant site on the catalyst

- X_3 is palmitic acid attached to the catalyst

- X_4 is the methanol

- X_5 is palmitic acid methyl ester attached to the catalyst

- $X_6$is water

- $X_7$is palmitic acid methyl ester

In step 5, the state vectors (ν_j) of reactions 1 to 6 are:

$$\nu_1 = \begin{bmatrix} -1 \\ -1 \\ 1 \\ 0 \\ 0 \\ 0 \\ 0 \end{bmatrix} \quad \nu_2 = \begin{bmatrix} 1 \\ 1 \\ -1 \\ 0 \\ 0 \\ 0 \\ 0 \end{bmatrix} \quad \nu_3 = \begin{bmatrix} 0 \\ 0 \\ -1 \\ -1 \\ 1 \\ 1 \\ 0 \end{bmatrix} \quad \nu_4 = \begin{bmatrix} 0 \\ 0 \\ 1 \\ 1 \\ -1 \\ -1 \\ 0 \end{bmatrix} \quad \nu_5 = \begin{bmatrix} 0 \\ 1 \\ 0 \\ 0 \\ -1 \\ 0 \\ 1 \end{bmatrix} \quad \nu_6 = \begin{bmatrix} 0 \\ -1 \\ 0 \\ 0 \\ 1 \\ 0 \\ -1 \end{bmatrix}$$

There is a link between deterministic and stochastic simulation. The rate constant (cj) for stochastic simulation can be calculated from kinetic parameters (k_j) in the deterministic simulation as illustrated below:

$$C_1 = \frac{k_1}{n_A vol}, \quad C_2 = k_2, C_3 = \frac{k_3}{n_A vol}, \quad C_4 = \frac{k_4}{n_A vol}, \quad C_5 = k_5, \quad C_6 = \frac{k_6}{n_A vol}$$

In addition $K_{AM} = \frac{k_1}{k_2}$, $K_S = \frac{k_3}{k_4}$ and $K_{DB} = \frac{k_5}{k_6}$

The reaction parameters of palmitic acid esterification over SO_4/ZrO_2-550°C were then determined in Table 5.

Table 5: Reaction parameters determined by stochastic model on SO_4/ZrO_2-550°C

Temp (C)	k_1	k_2	k_3	k_4	k_5	k_6
40	0.30	0.5	1.28	304.04	4.02	2
60	0.80	3	6.55	337.84	1	0.5
80	1.14	8.5	6.92	74.88	4.54	0.5

Results of the stochastic simulations for SO_4/ZrO_2-550°C at different temperature are shown below:

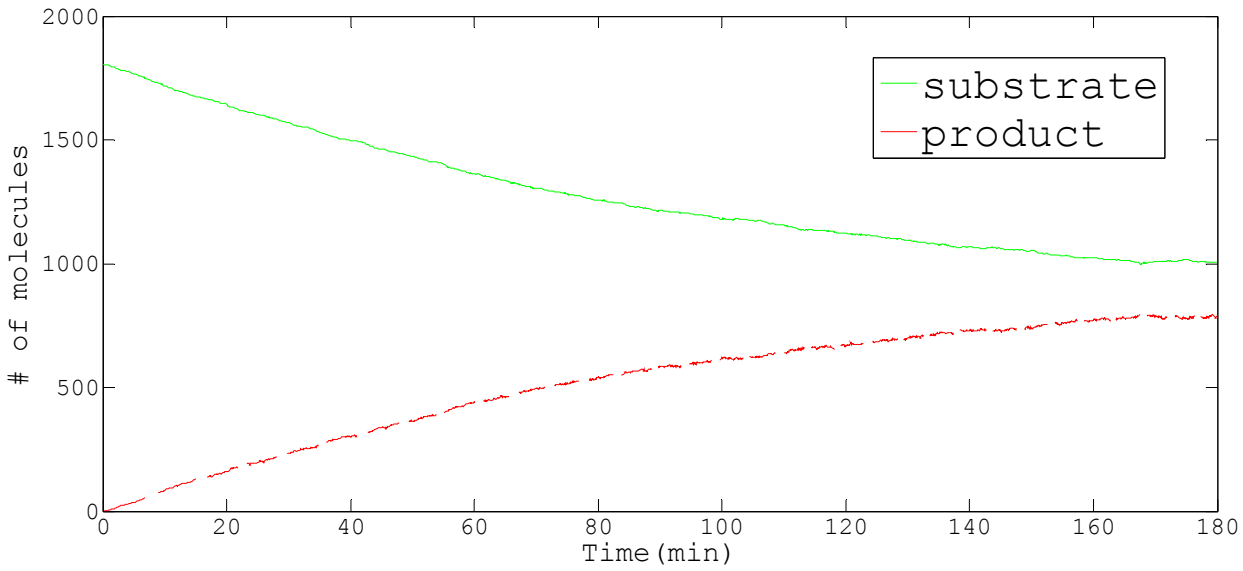

Figure 11: Stochastic simulation on SO_4/ZrO_2-550°C at 40°C

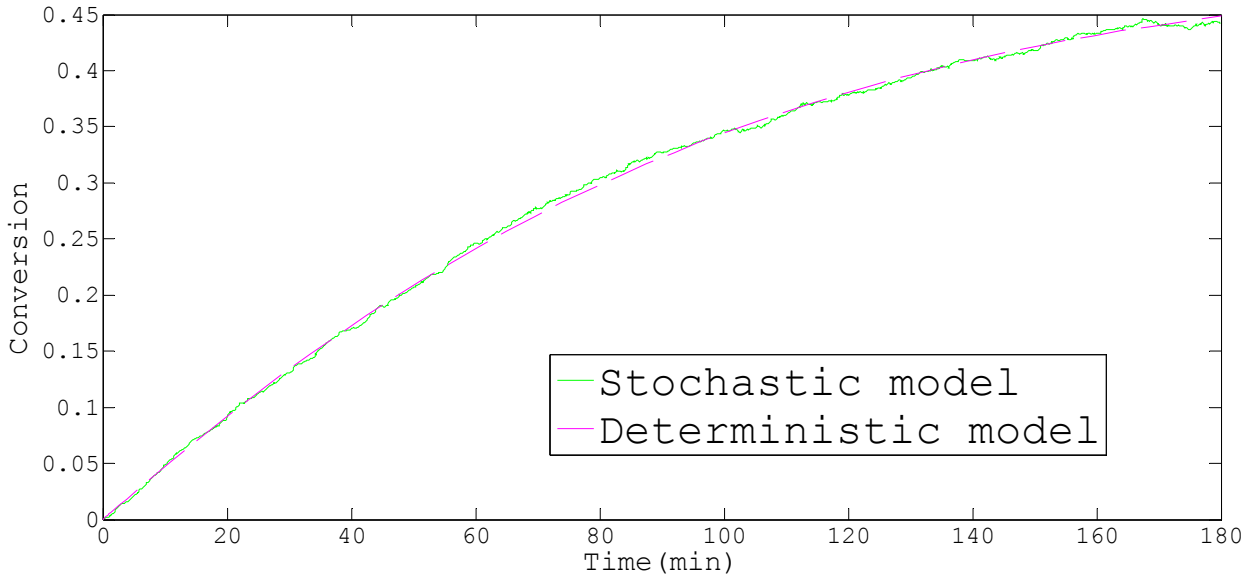

Figure 12: Comparison of Stochastic simulation vs. Deterministic model on SO_4/ZrO_2-550°C at 40°C

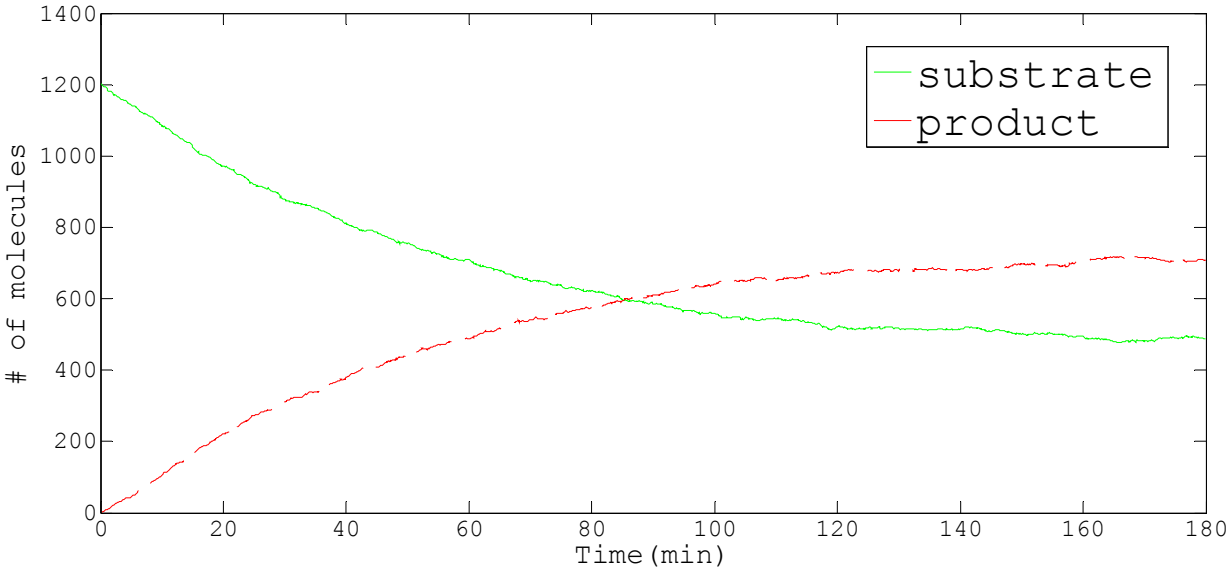

Figure 13: Stochastic simulation on SO_4/ZrO_2-550°C at 60°C

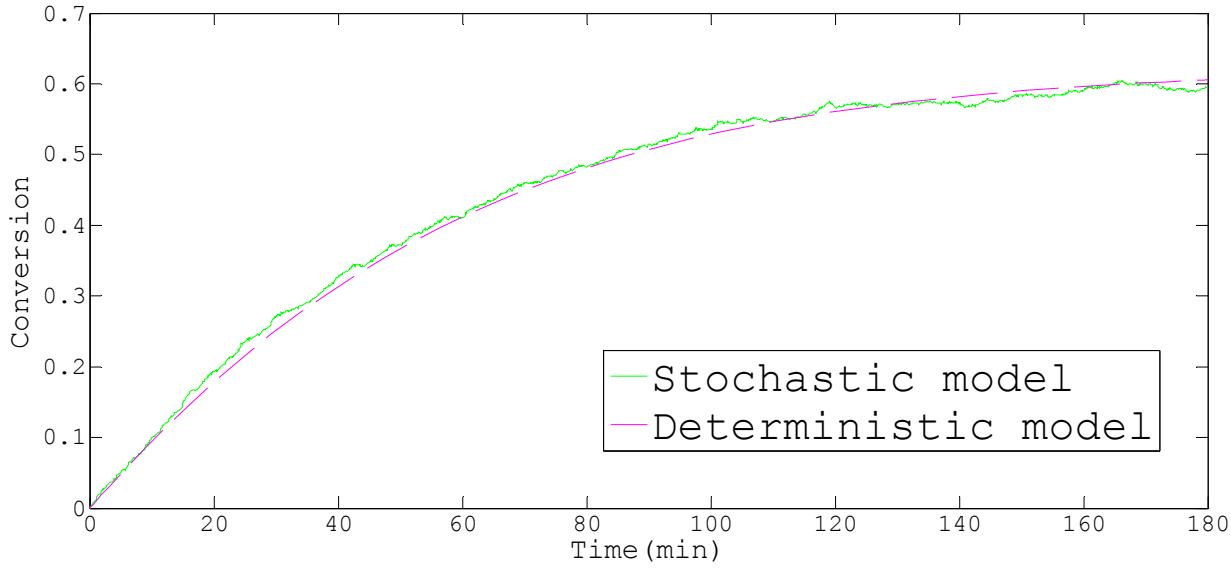

Figure 14: Comparison of Stochastic simulation vs. Deterministic model on SO_4/ZrO_2-550°C at 60°C

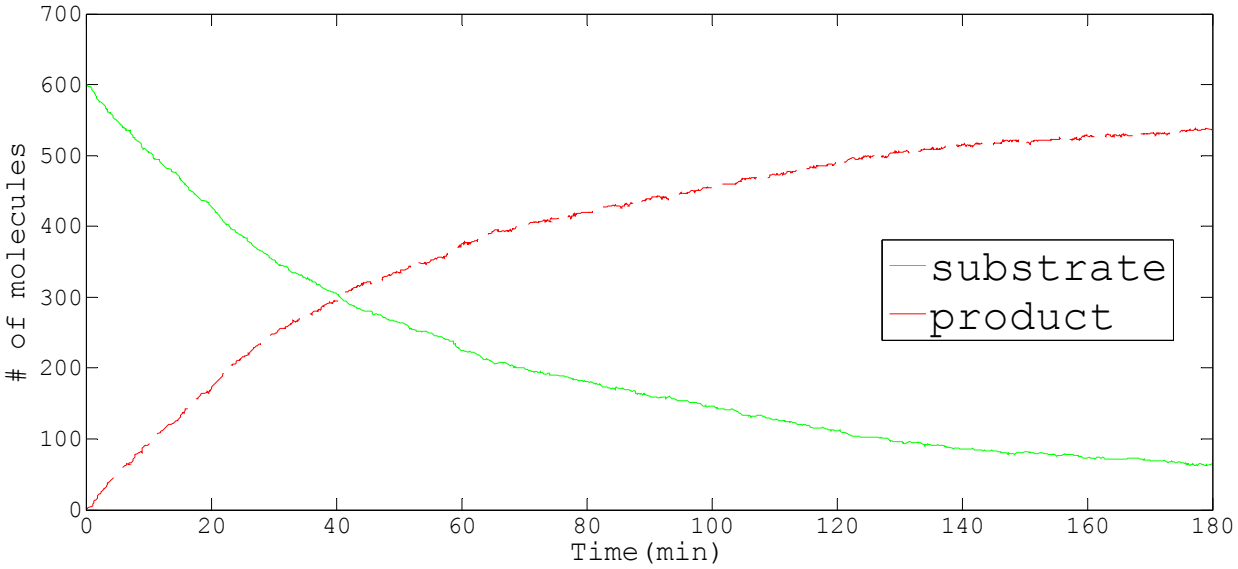

Figure 15: Stochastic simulation on SO_4/ZrO_2-550°C at 80°C

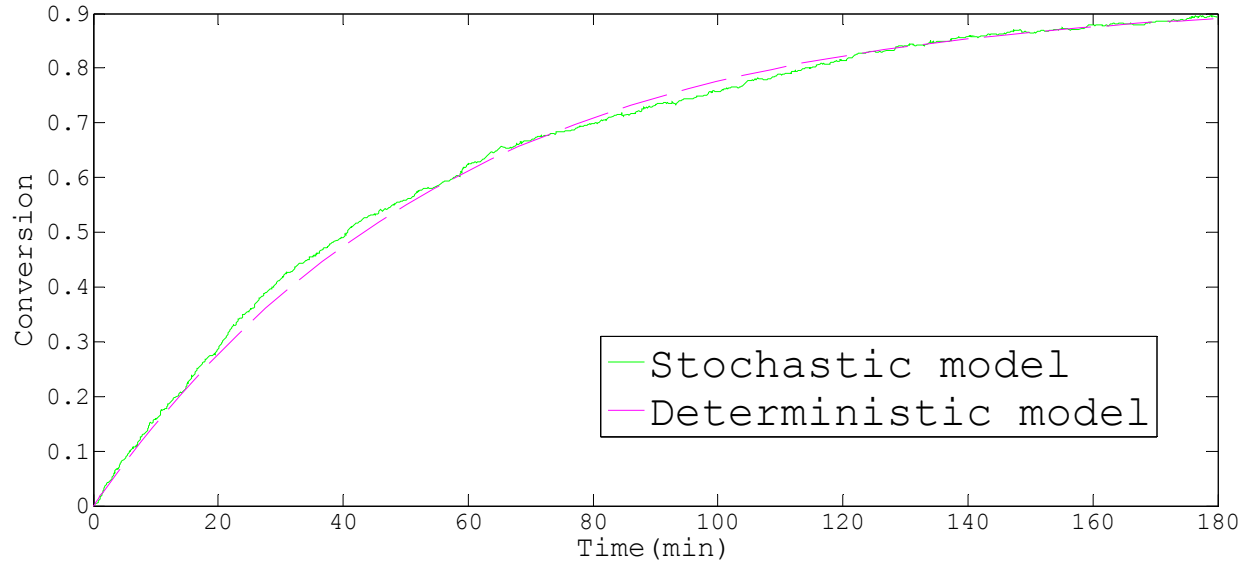

Figure 16: Comparison of Stochastic simulation vs. Deterministic model on SO_4/ZrO_2-550°C at 80°C

The stochastic simulation algorithms generated smooth graphs that are comparable to those produced in the deterministic model. However, the stochastic simulation generated smooth graphs as the

number of molecules in the system increased. The number of molecules employed were 1800, 1200 and 600 for SO_4/ZrO_2 at temperatures of 40, 60 and 80 ^{0}C, respectively. The stochastic simulation also further validated the Eley-Rideal mechanism over SO_4/ZrO_2 surface.

5.3 $AcAl_2O_3$ stochastic simulation

There are six sub-chemical reactions that occur during the esterification of palmitic acid over $AcAl_2O_3$. The solution contains seven species and X_n represents the n^{th} species. The six sub reactions are illustrated below:

1. $X_1 + X_2 \xrightarrow{C_1} X_3$ (1) $a_1 = C_1 X_1 X_2$

2. $X_3 \xrightarrow{C_2} X_1 + X_2$ (2) $a_2 = C_2 X_2$

3. $X_3 + X_4 \xrightarrow{C_3} X_5 + X_6$ (3) $a_3 = C_3 X_3 X_4$

4. $X_5 + X_6 \xrightarrow{C_4} X_3 + X_4$ (4) $a_4 = C_4 X_5 X_6$

5. $X_5 \xrightarrow{C_5} X_7 + X_2$ (5) $a_5 = C_5 X_5$

6. $X_2 + X_7 \xrightarrow{C_6} X_5$ (6) $a_6 = C_6 X_2 X_7$

Here,

- X_1 is methanol
- X_2 is vacant site of the catalyst
- X_3 is methanol attached on catalyst

- X_4 is pal mitic acid

- X_5 is palmitic acid methyl ester and methanol intermediate adsorbed on the catalyst

- X_6 is palmitic acid methyl ester

- X_7 is water

The rate constant (cj) for stochastic simulation can be calculated from kinetic parameters (k_j) in the deterministic simulation as illustrated below:

$$C_1 = \frac{k_1}{n_A vol},\ C_2 = k_2, C_3 = \frac{k_3}{n_A vol}\ ,\ C_4 = \frac{k_4}{n_A vol},\ C_5 = k_5,\ C_6 = \frac{k_6}{n_A vol}$$

In addition $K_{AM} = \frac{k_1}{k_2}$, $K_S = \frac{k_3}{k_4}$ and $K_{DB} = \frac{k_5}{k_6}$

The reaction parameters of palmitic acid esterification over SO_4/ZrO_2-550°C were then determined in Table 6.

Table 6: Reaction parameters determined by stochastic model on $AcAl_2O_3$

Temp (C)	$k_1 \times 10^{-2}$	$k_2 \times 10^{-3}$	k_3	k_4	k_5	k_6
40	1.89	0.94	9.70	500.00	1.19	0.55
60	1.27	9.10	6.23	300.00	16.08	8.00
80	2.08	271.59	10.82	95.00	20.10	10.00

Results of stochastic simulations for Alumina at different temperature are shown below:

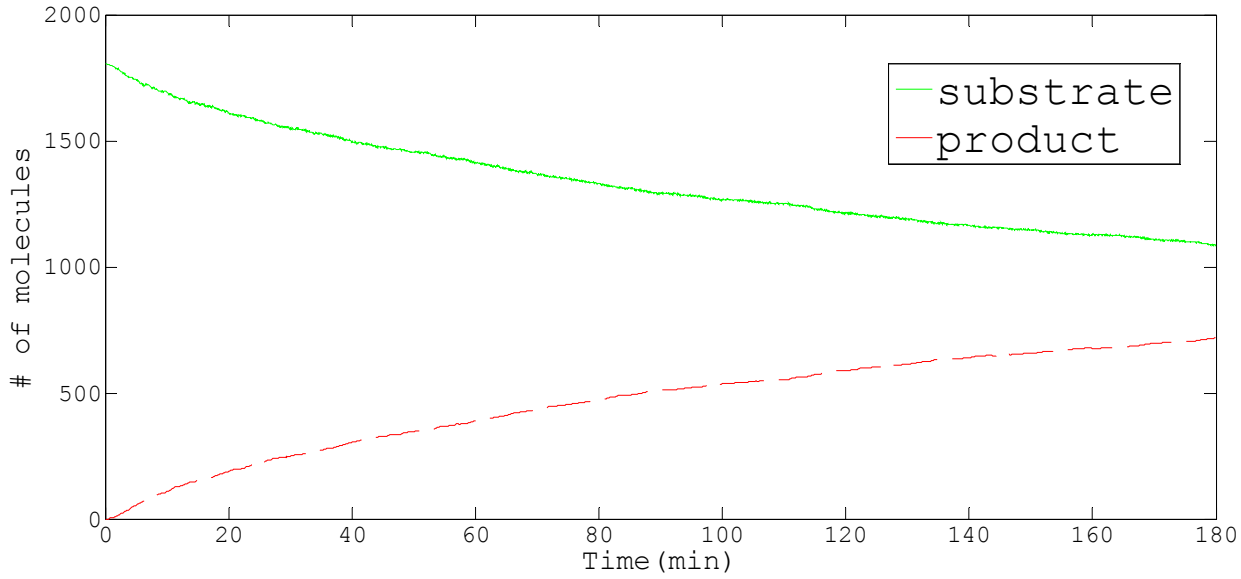

Figure 17: Stochastic simulation on $AcAl_2O_3$ at 40°C

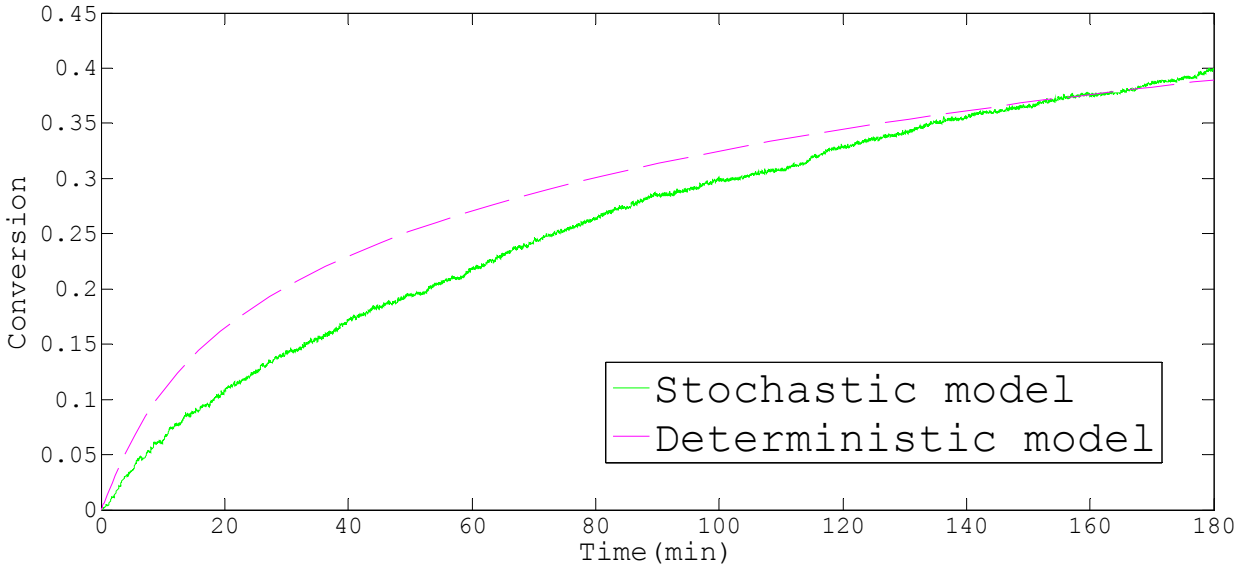

Figure 18: Comparison of Stochastic simulation vs. Deterministic model on $AcAl_2O_3$ at 40°C

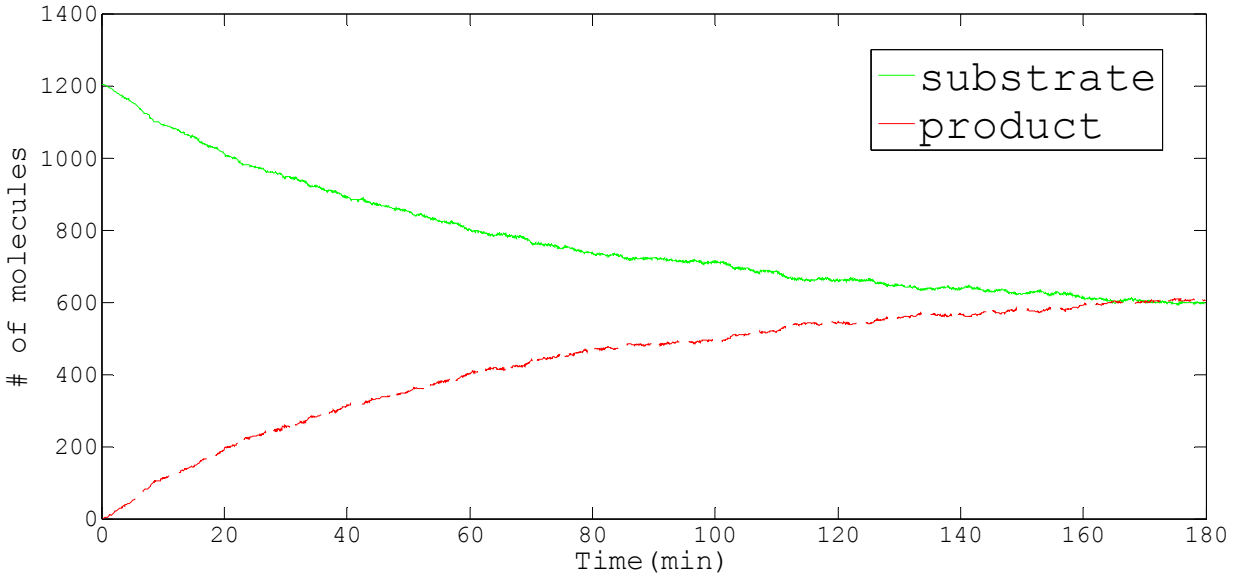

Figure 19: Stochastic simulation on $AcAl_2O_3$ at 60°C

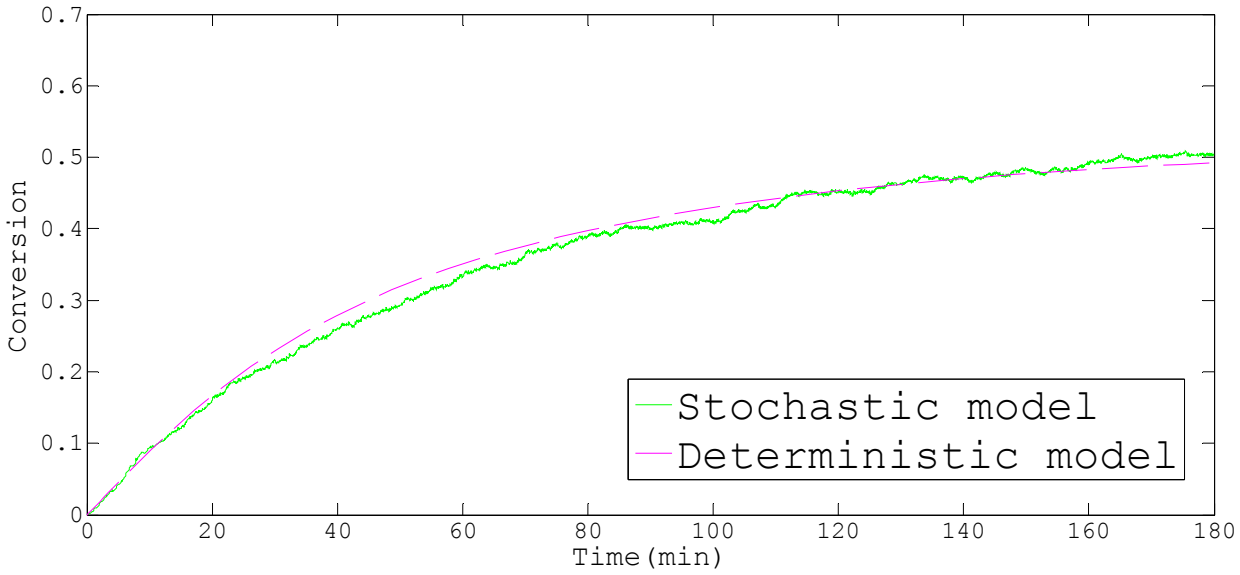

Figure 20: Comparison of Stochastic simulation vs. Deterministic model on $AcAl_2O_3$ at 60°C

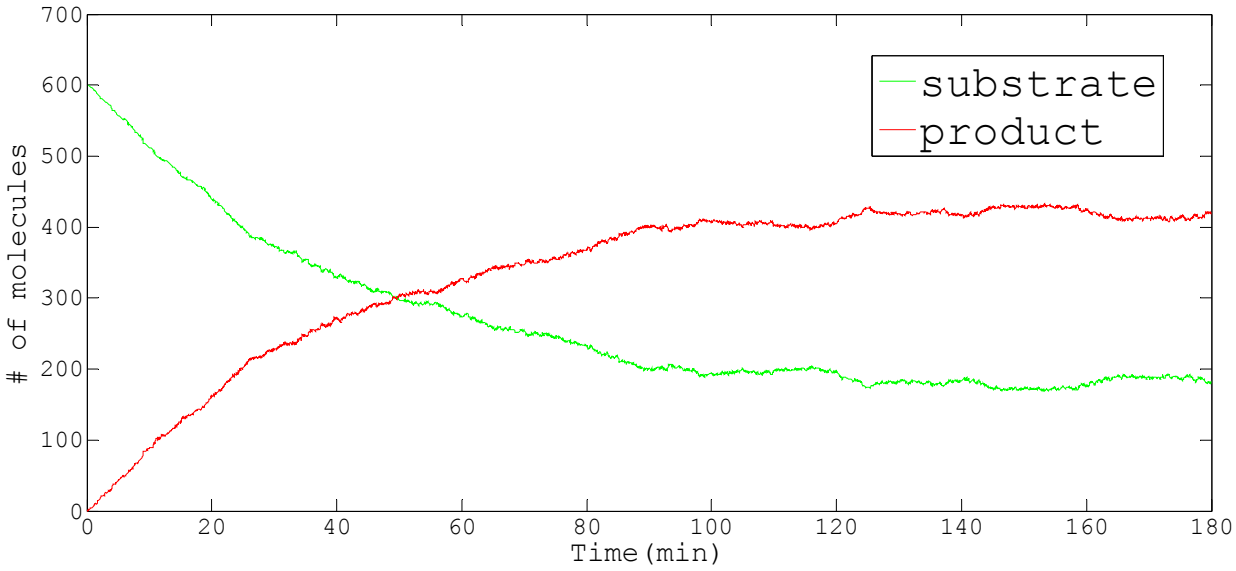

Figure 21: Stochastic simulation on $AcAl_2O_3$ at 80°C

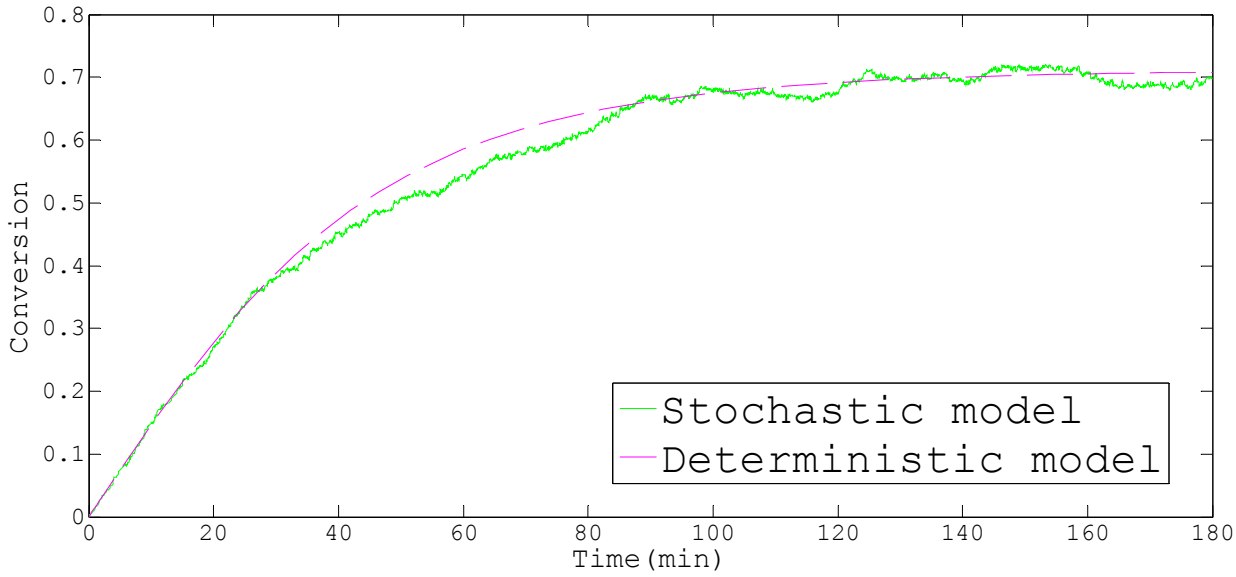

Figure 22: Comparison of Stochastic simulation vs. Deterministic model on $AcAl_2O_3$ at 80°C

The stochastic simulation generated smooth graphs as the number of molecules in the system increased. The number of molecules employed were 1800, 1200 and 600 for $AcAl_2O_3$ at

temperatures of 40, 60 and 80 ^{0}C, respectively. The stochastic simulation also further validated the Eley-Rideal mechanism over $AcAl_2O_3$ surface.

5.4 Discussion

The stochastic simulation is used as a tool for observing the nature of the reaction which occurs over the surface of the catalysts. The major difference at the molecular level between deterministic and stochastic is that the deterministic model mimics the experimental result whereas the stochastic model investigates the intrinsic nature of the reaction. The deterministic model does not take into account the stochastic nature of the chemical reaction. In a chemical reaction each individual reaction is an event that occurs with a certain probability. Practically, the deterministic model is easier to set up and faster in terms of calculation compared to the stochastic model. The deterministic model however, is not adequate at describing the intrinsic nature of chemical reactions. In order to observe the reactions which occur over the surface of the catalyst, a small number of molecules in the system will be observed. When dealing with a small number of molecules, the deterministic model cannot be used. In some systems such as biological processes, the reaction can be accurately simulated using a stochastic simulation.

In this thesis, the stochastic simulation algorithms generated smooth graphs that were comparable to those produced by the deterministic model. However, the stochastic simulation

generated smooth graphs as the number of molecules in the system increased. This was also observed as the temperature increased due to the increased frequency of collision and therefore there is a higher likelihood of reaction. The number of molecules employed were 1800, 1200 and 600 for both SO_4/ZrO_2 and $AcAl_2O_3$ at temperatures of 40, 60 and 80 ^{0}C, respectively. The stochastic simulation also further verifies the Eley-Rideal mechanism. The deterministic behavior represents the average of all these possible stochastic evolutions. Thus we note that the deterministic model and stochastic simulation are very close as illustrated in Figure 11 through 22 for both catalysts. Consequently, the deterministic result should be enough to describe the mechanism of the system. However, for other more complex catalyst, such as enzyme, the stochastic simulation could be essential in investigating the reaction mechanisms.

Chapter 6 Conclusions

Our results show that Eley-Rideal mechanism is appropriate to explain the reaction mechanism which occurs in the esterification of palmitic acid over both, SO_4/ZrO_2-550°C, and $AcAl_2O_3$. The reaction of adsorbed palmitic acid with methanol in bulk fluid is the rate-determining step for SO_4/ZrO_2-550°C. On the other hand, the adsorption of methanol on an active site on the catalyst was the rate-determining step in $AcAl_2O_3$. This difference in adsorbed species is attributed to the nature of the acid sites: SO_4/ZrO_2-550°C has mostly Brönsted acid sites whereas, $AcAl_2O_3$ has Lewis acid sites. Furthermore, the deterministic model and the stochastic simulation are in good agreement. It is therefore sufficient to use the deterministic model for the future kinetic investigation of free fatty esterification over heterogeneous catalysts. Furthermore, we showed that these models can be used to predict the conversion for different times. The heat of the reaction of SO_4/ZrO_2-550°C is 70.81 kJ/mol while that of $AcAl_2O_3$ is 93.70 kJ/mol indicating that SO_4/ZrO_2-550°C is better in the esterification for free fatty acids. Finally, this investigation of the esterification of free fatty acids serves as a model for further kinetic studies of transesterification of vegetable oil to biodiesel. Moreover, the combination of deterministic modeling and stochastic simulation can be used as a model to study more complex catalyst such as enzyme catalyst.

Appendix A: Nomenclature

A	Palmitic acid
E	Palmitic acid methyl ester
M	Methanol
S	Catalyst active site
W	Water
C_T	Total catalyst active sites
AS	Palmitic acid adsorbed on an active site
ES	Intermediate palmitic acid methyl ester on the catalyst surface
C_A	Concentration of palmitic acid, M
C_B	Concentration of methanol, M
C_E	Concentration of palmitic acid methyl ester, M
C_W	Concentration of water, M
C_{A0}	Initial concentration of palmitic acid, M
K_{AB}	Adsorption parameter of palmitic acid, $\frac{dm^3}{mol}$
K_{DB}	Desorption parameter of palmitic acid, $\frac{mol}{dm^3}$
K_{AM}	Adsorption parameter of methanol, $\frac{dm^3}{mol}$

K_s	Reaction rate constant, $K_s = \frac{k_{-s}}{k_s}$
k_{-s}	Kinetic constants of the forward reaction, $\frac{dm^3}{g_{cat}\, min}$
k_s	Kinetic constants of the reverse reaction, $\frac{dm^3}{g_{cat}\, min}$
X	Conversion of palmitic acid

Appendix B: Esterification of palmitic acid on SO_4/ZrO_2-550°C

Time (min)	Temperature (oC)	% catalyst loading (w/w)	Xa	Std Dev	[Ca], mol/l	[Cb], mol/l	[Cc], mol/l	[Cd], mol/l
0	40°C	10	0.0000	0.0185	0.2465	24.7129	0.0000	0.0000
30			0.1370	0.0422	0.2250	24.6914	0.0215	0.0215
40			0.1619	0.0705	0.2085	24.6749	0.0379	0.0379
50			0.2041	0.0663	0.1961	24.6625	0.0504	0.0504
60			0.2044	0.0783	0.1623	24.6287	0.0842	0.0842
80			0.3414	0.0783	0.1608	24.6272	0.0857	0.0857
100			0.3360	0.0231	0.1608	24.6272	0.0857	0.0857
140			0.4020	0.0478	0.1474	24.6138	0.0991	0.0991
180			0.4335	0.0361	0.1396	24.6060	0.1069	0.1069
0	60°C	10	0.0000	0.0000	0.2465	24.7129	0.0000	0.0000
20			0.1680	0.0748	0.2051	24.6714	0.0414	0.0414
40			0.2910	0.0396	0.1747	24.6411	0.0717	0.0717
60			0.4309	0.0478	0.1403	24.6066	0.1062	0.1062
80			0.4875	0.0281	0.1263	24.5927	0.1202	0.1202
110			0.5551	0.0190	0.1097	24.5760	0.1368	0.1368
140			0.5767	0.0483	0.1043	24.5707	0.1421	0.1421
180			0.6014	0.0318	0.0982	24.5646	0.1482	0.1482
0	80°C	10	0.0000	0.0000	0.2465	24.7129	0.0000	0.0000
20			0.2597	0.0367	0.1825	24.6489	0.0640	0.0640
30			0.3338	0.0870	0.1642	24.6306	0.0823	0.0823
40			0.5083	0.0371	0.1212	24.5876	0.1253	0.1253
60			0.6540	0.0656	0.0853	24.5517	0.1612	0.1612
80			0.7083	0.0100	0.0719	24.5383	0.1746	0.1746
120			0.8426	0.0085	0.0388	24.5052	0.2077	0.2077
180			0.8729	0.0159	0.0313	24.4977	0.2151	0.2151

Appendix C: Esterification of palmitic acid on $AcAl_2O_3$

Time (min)	Temperature, K	Temperature (oC)	% catalyst loading (w/w)	Xa	Std Dev	[Ca], mol/l	[Cb], mol/l	[Cc], mol/l	[Cd], mol/l
0	313K	40°C	100	0.00	0.0000	0.2465	24.7129	0.0000	0.0000
20				0.17	0.0093	0.2042	24.6706	0.0423	0.0423
40				0.24	0.0187	0.1877	24.6541	0.0587	0.0587
60				0.25	0.0080	0.1844	24.6507	0.0621	0.0621
90				0.29	0.0174	0.1743	24.6406	0.0722	0.0722
120				0.35	0.0108	0.1604	24.6268	0.0861	0.0861
130				0.36	0.0514	0.1575	24.6239	0.0889	0.0889
180				0.39	0.0041	0.1514	24.6178	0.0950	0.0950
0	333K	60°C	100	0.00	0.0000	0.2465	24.7129	0.0000	0.0000
10				0.17	0.0995	0.2055	24.6719	0.0410	0.0410
20				0.20	0.0553	0.1962	24.6626	0.0502	0.0502
50				0.31	0.0708	0.1706	24.6370	0.0758	0.0758
70				0.39	0.0757	0.1509	24.6172	0.0956	0.0956
120				0.45	0.0605	0.1365	24.6029	0.1099	0.1099
180				0.47	0.0175	0.1301	24.5965	0.1163	0.1163
0	353K	80°C	100	0.00	0.0000	0.2465	24.7129	0.0000	0.0000
20				0.29	0.0762	0.1740	24.6404	0.0725	0.0725
30				0.43	0.0592	0.1393	24.6057	0.1072	0.1072
40				0.48	0.0360	0.1281	24.5945	0.1184	0.1184
60				0.55	0.0166	0.1098	24.5762	0.1367	0.1367
80				0.59	0.0250	0.1007	24.5671	0.1458	0.1458
120				0.66	0.0313	0.0842	24.5505	0.1623	0.1623
180				0.71	0.0256	0.0716	24.5380	0.1748	0.1748

Appendix D: Experimental data for esterification of FFA on SO_4/ZrO_2-550°C for verifying model

Temperature	Time	Xa	Deviation
40°C	210min	0.4649	0.0455
	240min	0.4926	0.0469
60°C	210min	0.6175	0.0146
	240min	0.6330	0.0144
80°C	210min	0.9160	0.0094
	240min	0.9230	0.0048

Appendix E: Result of esterification from experiment for $AcAl_2O_3$ for verifying model

Temp, oC	time,min	X	Deviation
40	210	0.4387	0.0245
	240	0.4358	0.04
60	210	0.5211	0.0253
	240	0.5739	0.0251
80	210	0.7281	0.0446
	240	0.7572	0.0061

References

[Anon], Filtered Used Frying Fat Powers Diesel Fleet. *J Am Oil Chem Soc* 1982, *59* (10), A780-A781.

Adams, C.; Peters, J.; Rand, M.; Schroer, B.; Ziemke, M., Investigation of soybean oil as a diesel fuel extender: Endurance tests. *Journal of the American Oil Chemists' Society* 1983, *60* (8), 1574-1579.

Alencar, J. W.; Alves, P. B.; Craveiro, A. A., Pyrolysis of Tropical Vegetable-Oils. *J Agr Food Chem* 1983, *31* (6), 1268-1270.

Amenomiya, Y.; Cvetanovic, R. J., Active sites of alumina and silica-alumina as observed by temperature programmed desorption. *Journal of Catalysis* 1970, *18* (3), 329-337.

Arata, K., Preparation of Solid Superacid Catalysts. *Sekiyu Gakkaishi* 1996, *39* (3), 185-193.

Bartholomew, D., Viewpoint. *Journal of the American Oil Chemists' Society* 1981, *58* (4), 286A-288A.

Billaud, F.; Dominguez, V.; Broutin, P.; Busson, C., Production of Hydrocarbons by Pyrolysis of Methyl-Esters from Rapeseed Oil. *J Am Oil Chem Soc* 1995, *72* (10), 1149-1154.

Brito, A.; Borges, M. E.; Arvelo, R.; Garcia, F.; Diaz, M. C.; Otero, N., Reuse of Fried Oil to Obtain Biodiesel: Zeolites Y as a Catalyst. The Berkeley Electronic Press: 2007.

Crossley, A.; Heyes, T.; Hudson, B., The effect of heat on pure triglycerides. *Journal of the American Oil Chemists' Society* 1962, *39* (1), 9-14.

de Levie, R., Stochastics, the basis of chemical dynamics. *J Chem Educ* 2000, *77* (6), 771-774.

Di Serio, M.; Cozzolino, M.; Giordano, M.; Tesser, R.; Patrono, P.; Santacesaria, E., From Homogeneous to Heterogeneous Catalysts in Biodiesel Production. *Ind Eng Chem Res* 2007, *46* (20), 6379-6384.

Di Serio, M.; Tesser, R.; Dimiccoli, M.; Cammarota, F.; Nastasi, M.; Santacesaria, E., Synthesis of biodiesel via homogeneous Lewis acid catalyst. *Journal of Molecular Catalysis A: Chemical* 2005, *239* (1-2), 111-115.

Fjerbaek, L.; Christensen, K. V.; Norddahl, B., A Review of the Current State of Biodiesel Production Using Enzymatic Transesterification. *Biotechnol Bioeng* 2009, *102* (5), 1298-1315.

Fogler, H. S., *Elements of chemical reaction engineering*. 4th ed.; Prentice Hall PTR: Upper Saddle River, NJ, 2006; p xxxii, 1080 p.

Gillespie, D. T., Stochastic simulation of chemical kinetics. *Annu Rev Phys Chem* 2007, *58*, 35-55.

Gomes, J. F.; Puna, J. F.; Bordado, J.; Correia, M. J. N., Development of heterogeneous catalysts for transesterification of triglycerides. *React Kinet Catal L* 2008, *95* (2), 273-279.

Higham, D. J., Modeling and Simulating Chemical Reactions. *SIAM Review* 2008, *50* (2), 347-368.

Kiss, A.; Omota, F.; Dimian, A.; Rothenberg, G., The heterogeneous advantage: biodiesel by catalytic reactive distillation. *Top Catal* 2006, *40* (1), 141-150.

Kulkarni, M. G.; Dalai, A. K., Waste Cooking OilAn Economical Source for Biodiesel: A Review. *Ind Eng Chem Res* 2006, *45* (9), 2901-2913.

Kulkarni, M. G.; Gopinath, R.; Meher, L. C.; Dalai, A. K., Solid acid catalyzed biodiesel production by simultaneous esterification and transesterification. *Green Chemistry* 2006, *8* (12), 1056-1062.

Lotero, E.; Liu, Y.; Lopez, D. E.; Suwannakarn, K.; Bruce, D. A.; Goodwin, J. G., Synthesis of Biodiesel via Acid Catalysis. *Ind Eng Chem Res* 2005, *44* (14), 5353-5363.

Ma, F. R.; Hanna, M. A., Biodiesel production: a review. *Bioresource Technol* 1999, *70* (1), 1-15.

Mira, J.; Fenandez, C. G.; Urreaga, J. M., Two examples of deterministic versus stochastic modeling of chemical reactions. *J Chem Educ* 2003, *80* (12), 1488-1493.

Pasias, S.; Barakos, N.; Alexopoulos, C.; Papayannakos, N., Heterogeneously Catalyzed Esterification of FFAs in Vegetable Oils. *Chemical Engineering & Technology* 2006, *29* (11), 1365-1371.

Perin, D.; Armareg, W.; Perrin, P. In *Heterogeneous Catalysis in the transesterification of mamona and soy oils*, Proceedings of 29th Annual Reunion of Chemical Brazilian Society, Brazil, 2006.

Peterson, C. L.; Auld, D. L.; Korus, R. A., Winter Rape Oil Fuel for Diesel-Engines - Recovery and Utilization. *J Am Oil Chem Soc* 1983, *60* (8), 1579-1587.

Pryde, E., Vegetable oils as diesel fuels: Overview. *Journal of the American Oil Chemists' Society* 1983, *60* (8), 1557-1558.

Rosa, M.; Oliveira, A. In *Synthesization of Biodiesel by Tin (IV) complexes*, Proceedings of the 3rd Brazilian Congress of Petroleum and Gas, Brazilian Petroleum and Gas Institute: Brazil, 2005.

Rosa, M.; Oliveira, A. In *Carbonates utilization as heterogeneous catalysts of transesterification*, Proceedings of 29th Annual Reunion of Chemical Brazilian Society, Brazil, 2006.

Santos, A. Heterogeneous Catalysts for Biodiesel production – Metanolysis of Soy Oil over Hidrotalcytes of Magnesium and Aluminium changed. IST/UTL, Lisbon, 2007.

Schwab, A.; Dykstra, G.; Selke, E.; Sorenson, S.; Pryde, E., Diesel fuel from thermal decomposition of soybean oil. *Journal of the American Oil Chemists' Society* 1988, *65* (11), 1781-1786.

Schwab, A. W.; Bagby, M. O.; Freedman, B., Preparation and Properties of Diesel Fuels from Vegetable-Oils. *Fuel* 1987, *66* (10), 1372-1378.

Shafiee, S.; Topal, E., When will fossil fuel reserves be diminished? *Energy Policy* 2009, *37* (1), 181-189.

Shay, E. G., Diesel Fuel from Vegetable-Oils - Status and Opportunities. *Biomass Bioenerg* 1993, *4* (4), 227-242.

Srivastava, R.; Srinivas, D.; Ratnasamy, P., Fe-Zn double-metal cyanide complexes as novel, solid transesterification catalysts. *Journal of Catalysis* 2006, *241* (1), 34-44.

Vicente, G.; Martínez, M.; Aracil, J., Integrated biodiesel production: a comparison of different homogeneous catalysts systems. *Bioresource Technol* 2004, *92* (3), 297-305.

WEISZ, P. B.; HAAG, W. O.; RODEWALD, P. G., Catalytic Production of High-Grade Fuel (Gasoline) from Biomass Compounds by Shape-Selective Catalysis. *Science* 1979, *206* (4414), 57-58.

West, A. H.; Posarac, D.; Ellis, N., Simulation, case studies and optimization of a biodiesel process with a solid acid catalyst. *Int J Chem React Eng* 2007, *5*, -.

Zhang, Y.; Dubé, M. A.; McLean, D. D.; Kates, M., Biodiesel production from waste cooking oil: 1. Process design and technological assessment. *Bioresource Technol* 2003, *89* (1), 1-16.

Ziejewski, M.; Kaufman, K. R.; Schwab, A. W.; Pryde, E. H., Diesel-Engine Evaluation of a Nonionic Sunflower Oil Aqueous-Ethanol Microemulsion. *J Am Oil Chem Soc* 1984, *61* (10), 1620-1626.